

Master's Thesis

Master in energy engineering

Wind turbine modelling for lightning simulations.

REPORT

Author: Alejandro Cao Faci
Director: Joan Montanyà Puig
Co-director: Jesús Alberto López Trujillo
Convocation: September 2018



Escola Tècnica Superior
d'Enginyeria Industrial de Barcelona



ABSTRACT

The present project proposes a wind turbine model for studies about its effects with reference to lightning strikes. For this, a meticulous compilation of high frequency models of each element of a conventional wind turbine has been carried out in order to select the most suitable ones. Subsequently, these models have been introduced in the ATPDraw software to perform the relevant simulations.

In parallel, due to the absence of models about the power converter in the available literature, we have tried to model it and obtain an equivalent circuit that could reflect its behaviour in lightning tests. To do this, a series of experiments were carried out using a pulse generator and real equipment to obtain tangible information about its behaviour and, then, some tests were carried out with different models until finding one that offered the adequate operation.

Finally, all previously evaluated models are introduced into the ATPDraw forming a wind turbine, and an impulse similar to that of a standard lightning is applied. In this way, it is possible to study which is the overall behaviour of the whole system and specifically, about each element presented to obtain the final conclusions. As a whole, it can be said that a relatively simple system is obtained that offers a performance very similar to the reality one.

INDEX

ABSTRACT.....	1
INDEX	2
1. GLOSSARY	4
2. INTRODUCTION.....	5
2.1 OBJECTIVES	6
3. OVERVOLTAGES IN WIND TURBINES.....	8
3.1 Overvoltages analysis in wind farms	10
3.2 Behaviour of the main wind turbine's elements under overvoltages.....	12
3.2.1 Transformer behaviour under overvoltages.....	14
3.2.2 Generator behaviour under overvoltages	17
3.2.3 Power converter behaviour under overvoltages	19
3.3 TOV protection.....	20
4. MODELLING OF THE WIND TURBINES.....	24
4.1 Transformer modelling.....	24
4.2 Generator modelling	27
4.3 Power converter modelling	28
4.3.1 Real data getting	29
4.3.2 Models Review	31
4.3.3 Main improvements of model 2 to obtain 3.....	38
4.4 Other elements of the wind turbine.....	38
5. FINAL RESULTS.....	45
5.1 Wind farm characteristics	45
5.2 Simulation tools	46
5.2.1 Lightning current source simulation.....	47
5.2.2 Blades and tower simulation.....	48
5.2.3 Power cable system	49
5.3 Wind turbine Simulation.....	51
5.3.1 Evaluation of the overvoltages including a surge arrester	56
5.4 Limitations and possible improvements of the project	57

6. CONCLUSIONS	59
7. BIBLIOGRAPHY	60
8. ANNEX I: TOOLS USED IN THE TESTS.....	63
9. ANNEX II: GRAPHICS OBTAINED IN THE TESTS.....	66
9.1 Test 1:.....	66
9.2 Test 2.....	69
9.3 Test 3.....	71
10. ANNEX III: COMPARISON BETWEEN THE TEST AND THE FINAL CONVERTER MODEL	74
10.1 Open circuit test:	74
10.2 Short-Circuit Test.	76
11. ANNEX IV: FINAL SIMULATION	78

1. GLOSSARY

In this section the meaning of the different abbreviations and symbols used along the project is specified:

Abbreviations

<i>AC</i>	Alternating Current.
<i>CP</i>	Constant Parameter.
<i>DC</i>	Direct Current.
<i>DFIG</i>	Doubly Fed Induction Generator.
<i>EHV</i>	Extra high voltage.
<i>FEM</i>	Finite Element Program.
<i>HV</i>	High Voltage.
<i>LPS</i>	Lightning Protection System.
<i>LV</i>	Low Voltage.
<i>MV</i>	Medium Voltage.
<i>OC</i>	Open Circuit.
<i>PWM</i>	Pulse-Width Modulation.
<i>SC</i>	Short-Circuit.
<i>THD</i>	Total Harmonic Distortion.
<i>TOV</i>	Transitory overvoltages.

Symbols

ϵ	Permittivity.
μ	Permeability
Ω	Ohm.
ρ	Resistivity.

2. INTRODUCTION

During the last years, the production of wind energy has been expanded all over the world, reaching an installed power worldwide of more than 486 MW in 2016, with such a growth that has doubled the power of 2011 [1]. In this way, wind energy is the most mature and developed renewable energy currently, being the one that generates more electricity behind hydroelectric power, using only the force of the wind as an energy source. In addition, its future is no less promising, since with the constant increase of the nominal power of the installed wind turbines and the increasing viability of offshore wind farms, it is believed that between solar and wind energy they could generate the 80% of the electricity demanded in some countries before 2030 [2].

Even so, this growing presence of the wind energy presents several challenges to bear in mind, apart from those already existing for being an energy source dependent on weather conditions. As will be discussed below, the project will study in depth the problem of overvoltages in wind turbines, and more specifically those produced by lightning.

The concept of overvoltage is referred to those voltage surges that can appear in electrical distribution lines, data, communications or telephony, causing premature deterioration of the components and damage the equipment connected to the network. In particular, the present project will study the incidence of transient overvoltages produced by direct, indirect atmospheric discharges, disconnection of inductive loads and network switching.

Specifically, the transients to study will be those caused by direct or indirect atmospheric discharges. The main reason for this, is the large amplitude and high frequency that a lightning can achieve, becoming dangerous even in an indirect impact. In some cases, they can reach around 100 kA with a frequency higher than 10^5 Hz.

Regarding the wind energy scenario, it must cover large areas of land to produce big amounts of energy. In this way, wind turbines are usually located in high places where the wind can be used, so the incident lightning strike is increased, causing adverse effects on the individual and common operation of wind turbines. The main reason for this is that they are structures that are very exposed to lightning and statistically, can initiate lightning very easily [3]. If they are not properly dissipated, it can lead to consequences on the physical condition of the wind turbine.

Then, the problem may seem very simple, only by placing the correspondent protections in the system, the consequences could be mitigated to a great extent. But, if the economic factor is taken into account, it is essential to know that a large investment is required. Consequently, it would be necessary to carry out the pertinent studies on each case and wind farm location, in order to evaluate the risks of the system and its vulnerability to those disturbances provoked by lightning strokes.

In this way, an important part of the present project will focus on analysing the most problematic overvoltages, with the aim of optimally modelling the main elements of wind turbines, both individually and in a wind farm. Therefore, the second part of the project will consist in compiling and studying the high frequency models of the most representative elements of a wind turbine.

At present, it is very difficult to find studies on high frequency models of the elements of a wind turbine. The reason for this, is that nowadays exist a set of standard models for each of them, and they are good approximations for almost any application in the industry. The main problem then, is that the classic models do not work for the high frequencies of the disturbances that appear during a temporary overvoltage, because important impedances can appear that for common applications are totally negligible.

In summary, it can be said that the motivation for the present study of the overvoltages produced by lightning in wind turbines, is based on different reasons. Firstly, we are facing a problem that affects many countries nowadays, and due to the increasing use of wind energy, it could be more frequent in the following years. In addition, the expansion of wind energy is a relative recent phenomenon, so the number of deep studies about the problem is limited. Apart from this, there does not exist a set of models in high frequency accepted for the community for all the elements of a wind turbine, even in the case of the converter there is a very limited bibliography about it.

2.1 OBJECTIVES

The main objective of the project is to obtain a complete model for lightning tests of a wind farm, and specifically of an individual wind turbine in the ATPDraw software. To do this, each and every one of the elements that composes a wind farm must be considered individually, bearing in mind the high frequencies that can appear owing to the overvoltages produced by lightning.

In addition, it is necessary to focus on the power converter model, because due to the absence of available literature, it is intended to obtain an own model that could be used in high voltage tests. At the end, the project will finish with a lightning simulation to evaluate the final results obtained, and its precision bearing in mind the time constraints, and the available software and bibliography. For this, the following previously established steps will be carried out:

1. Compilation of information on various related topics such as the characteristics of lightning, parts of wind turbines and their behaviour against overvoltages, and electrical protection against major disturbances.

2. Obtain different models of wind turbines and its main components to make a selection of the most precise bearing in mind the predefined objectives and the pertinent limitations.
3. To obtain the model of the converter, a series of tests will be carried out in a laboratory and later compared with the available models, modifying them if necessary to achieve a model that can reflect the corresponding overvoltages as much as possible.
4. Finally, once the previous steps have been completed, the aim is to unite all the models of the components in a single program in order to simulate a lightning and evaluate the final behaviour of the system.

3. OVERVOLTAGES IN WIND TURBINES

In this section, the behaviour of the different elements of a three-bladed wind turbine in front of lightning will be commented, since it is the type that is more present actually to generate large amounts of energy around the world. Afterwards, the effect of overvoltages in the transformer, the power converter and the generator will be analysed, since they are the most complex elements of the whole system.

In Fig. 1, we can see the main elements of a common three-bladed wind turbine, although there are different configurations depending on the chosen devices and their placement. Regarding the lightning strikes, each wind turbine whatever the configuration, must carry the current produced to ground. Accordingly, it is deduced that an access to ground is necessary for each wind turbine, although it may be complicated due to the rocky terrain where they can be located [3].

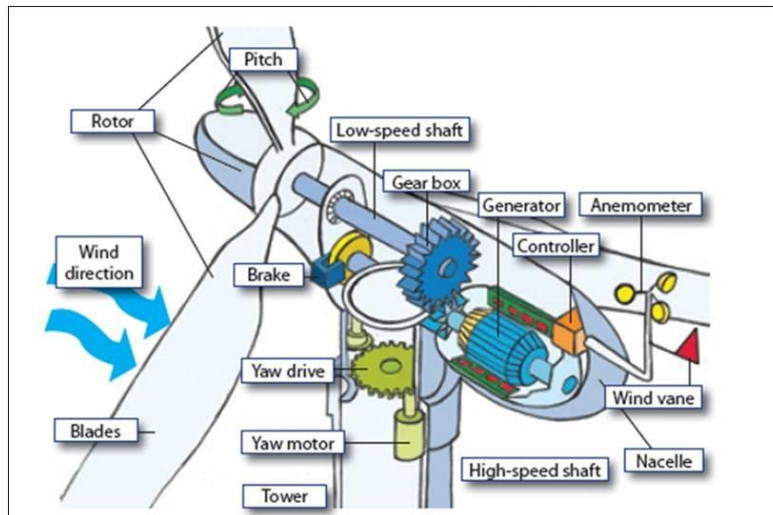


Fig. 1: Schematic overview of wind turbine components. Source: L.E.T.

Apart from this, according to [4] there are a huge quantity of lightning types e.g. positive and negative lightnings, cloud-to-ground lightning, ground-to-cloud lightning, intracloud lightning. Despite this, all of them are essentially the same, a channel of ionized air carrying electrical current between two differing areas of charge. Then, the most widespread protections for each component of the wind turbines and the main effects in each of these are presented. For the analysis, as can be seen on Fig. 1, the most common parts and dimensions of a three-bladed wind turbine are considered and therefore, the most susceptible to overvoltages due to lightning strikes and huge disturbances.

Blades

To start, it is necessary to highlight the blades of the wind turbines, since they are their most distinctive part and can reach heights of 200 m, making it the most susceptible part to receive lightning strikes. The main function of the blades is to extract the energy from the wind, transforming it into kinetic energy of rotation, which thanks to its connection to the hub by means of a ball bearing, allows it to rotate around its axis. The bearing is attached to the blade by its inner ring and the hub by the outside one.

At the moment, the materials of construction of the blades are very varied, although the most common are usually made of a matrix of fiberglass meshes impregnated with a material such as hardened polyester or epoxy. In this way the base matrix can be made, totally or partially, of carbon fiber, being a material with high strength and lightness, but more expensive. In large rotor blades, wood-epoxy sheet materials are also being used [5].

Even though depending on the material the consequences of a direct impact by a lightning can be mitigated, there can usually be found considerable erosions in the air terminals, shell punctures and tearing, and stripping of the materials of the blade [6]. In more extreme cases, blade breakdown or blade burnout and wire melting can occur. For this reason, it is important that the blades have a good lightning protection system (LPS) to safely drive those dangerous currents to the hub or nacelle. This is achieved through an air termination system, based on different configurations and is described in detail in [6].

Hub

The vast majority of the direct impacts of lightning on wind turbines occur in the blades, meaning that the current must be properly conducted to the ground, so there are some models that are responsible for transferring this current to the nacelle through the hub. This is mainly because the hub itself is not very susceptible to be damaged, since it is made of metal, but some inner systems could be deteriorated.

As a result, a set of methods has been developed to protect the hub from high currents, which are again listed in [6]. Among them, the most common are to implement the model of wind turbine that avoid the passage of current through the hub by spark gaps or brushed contacts between the root of the blade and the nacelle, by bonding all conductive components, bypassing pitch bearings and hydraulic actuators, shielding and installing overvoltage protection of wiring.

Nacelles

As for the nacelle, we are in a scenario very similar to the previous one, with the difference that it is an element manufactured with fiberglass as previously mentioned, so there is the obligation of installing an LPS. In addition, although statistically does not happen commonly, there exist the possibility that a direct impact against the nacelle happens, therefore we must protect the system by installing a mesh or fixing some air termination systems.

As a summary, simplifying the system considerably, it can be said that the main objective of the mentioned measurements is to safely drive the lightning currents from the top of the tower to the ground system, which in some cases can be represented as a low resistance [7]. The phenomenon is schematized in Fig. 2.

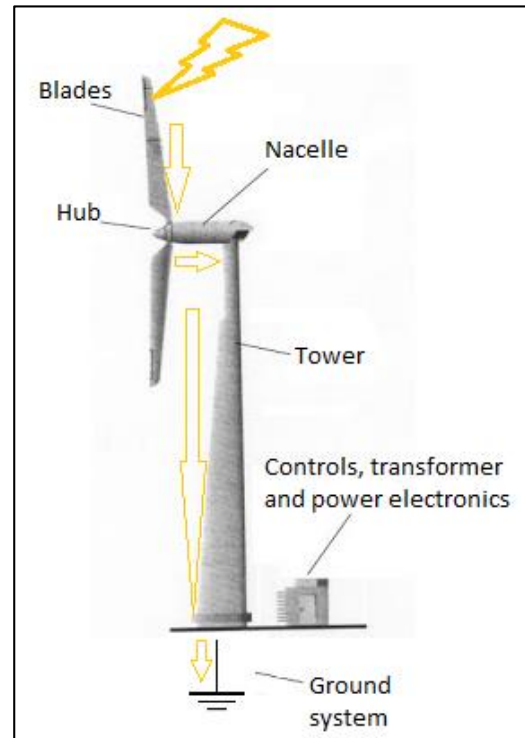


Fig. 2: Lightning behaviour in a wind turbine. Source:

<http://usefulproject.blogspot.com.es>

3.1 Overvoltages analysis in wind farms

Lightnings are a natural phenomenon which, influenced by several factors, occur most commonly in wind farms. In this way, the shaped current conduction directly origins overvoltages caused by voltage drops in the conductive elements, including the grounding system. These overvoltages can lead to a loss of insulation, and the malfunction of some systems [6]. In addition, both direct and indirect lightning impacts on wind turbines or transport and distribution lines can produce those transitory overvoltages (TOV), despite there are many factors that can influence the TOV impact e.g. soil resistivity, lightning characteristics, and distance to the conductors.

Currently, there are several events that can produce overvoltages in wind turbines, but the most risky can be those from the ground potential rise and the induced overvoltages due to magnetic fields [6]. In the same way, if a wind farm is considered globally, the overvoltage produced in one of the wind turbines, can affect the rest of them without the need of having been directly affected by a lightning strike.

Consequently, it is necessary to carry out an exhaustive analysis on the adequate protections against surges for each wind turbine in particular and for the wind farm in general. Furthermore, determining the lightning incidence of wind turbines is very complex,

for the peculiarities of being a tall structure in general, and specifically a wind turbine. Below are the most imperative factors to consider for a lightning surge analysis of a wind farm, presented in [8]:

Soil resistivity. The fact that wind turbines are usually located in rocky and mountainous places means that installing the necessary ground system is very expensive and a technological challenge for the designers. On the one hand, in case of a direct impact, the currents that circulate towards the ground can cause the overvoltages mentioned by the voltage drop of the ground resistance, and cause losses of insulation and damages in the systems. On the other hand, in case of an impact on the surface of the ground, the overvoltage can end up in the cables and again produce losses of insulation and damage to the systems, although it also depends on the distance of the lightning from the point of study.

Lightning characteristics. Choosing the appropriate protections for wind turbines is greatly complicated when this factor is taken into account, mainly because it is linked to the economic factor. The best solution from the technological point of view, would be simply to install some protections that could absorb the maximum possible energy, but for practical purposes, choosing that type of protection in a place where practically any lightning strike during the year would be illogical.

Therefore, the most usual procedure is to carry out a statistical study on the characteristics of the lightnings in the wind farm, and more specifically the lightning strike density. Then, the next step is to choose the optimal protection regarding its price, and the risk of system failure. It is explained deeply in [8].

Individual characteristics of the wind turbines. It is important to bear in mind that the characteristics of the individual equipment of each wind turbine and its disposition may have a huge impact when finding the suitable surge protections. With the reason that the electrical system of a wind turbine is very complex, the great impact that this factor could mean will be explained later in the project.

Wind farm topology. The topology of the electrical system of the wind farm affects to a large extent the magnitude of the TOV in some of the parts of the wind farm, in the same way as the disposition and calibration of the different protections to be implemented. As an example, it can be highlighted that the cascade connection between wind turbines means higher overvoltages than in the parallel configuration.

The main reason for the great importance of this factor, is that although it does not look like it, when the transient overvoltage appears a back-surge can occur. Then, from the ground system of the wind turbine that has suffered the TOV, the disturbance can be transferred to the phase conductors. Consequently, the

disturbance can spread through the ground system throughout the wind farm until it is finally dissipated by the available protections.

So, if all these factors are kept in mind, even driving the current safely to the ground, this circulation can cause an increase in the soil potential. Thus, this potential increase can produce large potential differences in many elements that are referenced to ground, such as the transformer, which under certain conditions can transfer the disturbance from the point of MV to the point of LV. In addition, the converter and the generator can transfer the TOV in a similar way, so they must also be taken into consideration.

In the same way, as can be seen in Fig.3, the lightning currents can induce electromagnetic forces by means of electromagnetic induction to the conductors.

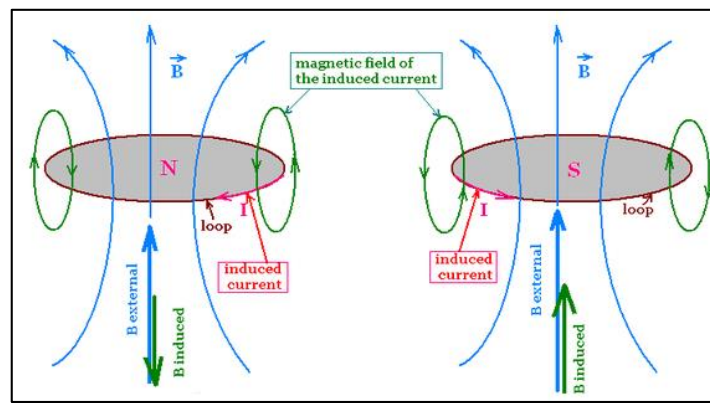


Fig. 3: Explanation of Faraday's law of induction. Source: Qurit Ulain, BS Physics from university of Sargodha (2017), "How exactly does Faraday's law relate to Lenz's law?"

3.2 Behaviour of the main wind turbine's elements under overvoltages.

Before reviewing what would be the appropriate model for the power transformer, the power converter and the generator of the wind turbine, in this section it will be studied the behaviour of these elements during an overvoltage, at a general level and later in a wind turbine specifically. As previously mentioned, overvoltages in the form of short and isolated impulses can be produced by different causes, but the most dangerous are usually those produced by atmospheric discharges. Then, to understand the effect of the overvoltages in each element, it is important to understand how the typical form of an overvoltage produced by a lightning is:

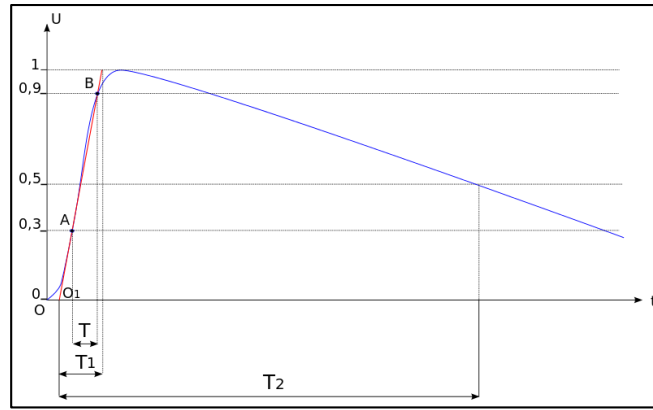


Fig. 4: Standard lightning impulse waveform. Source: Psemdel. February 2014.

In Fig 4, it can be seen the waveform of the voltage with respect to the most usual time of a lightning. The values of the voltage are established per unit for the reason that its magnitude, as we have seen previously, depends on a large number of parameters and can vary widely. On the other hand, focusing on the duration of the overvoltage, different important intervals of time can be observed to know its waveform [9]:

T: It is the period of time that elapses between the overvoltage passing from 30% to 90% of its maximum value. Although it depends on different characteristics, its value is around $0.6\text{--}0.8\ \mu\text{s}$.

T1: It is the period of time that passes from the beginning of the overvoltage until it reaches its maximum value. It usually lasts around $1.2 \pm 30\%\ \mu\text{s}$, and its value is equal to $1.67 \cdot T$.

T2: It is the period of time that passes from the beginning of the overvoltage until it reaches its maximum value and drops until its 50%. It usually lasts around $50 \pm 20\%\ \mu\text{s}$.

It can be seen that during the first moments of the overvoltage, which increases to its maximum value, it can look like a sinusoidal wave, being its period quarter $T1$. In other words, during $T1$ the voltage to which the winding is subjected is a sinusoidal wave of frequency $f = 1 / (4 \cdot T1)$ [10]. Once the maximum of the overvoltage has passed, its value starts to decrease gradually, so the distribution of the voltage is similar to what would be obtained with a continuous voltage during the microseconds the perturbation is still present.

In this way, it is important to design the different equipment and the adequate protections so that the system is able to resist this voltage without suffering deterioration [11] [12]. These are normally harmful to electrical equipment when its amplitude is greater than the insulation level for which the material is designed.

3.2.1 Transformer behaviour under overvoltages

A transformer generally has the same level of insulation as the rest of the installation's materials, but it is much more sensitive to overvoltages [13]. A transformer has a high input impedance and is a very sensitive component for wave reflection, so to limit the acceptable overvoltages, it is necessary to install the pertinent protections. The most widespread solution is to implement surge arresters as closer as possible to the connection points of the transformer [6].

The problem found then is that at such high frequencies ($\sim 10^5$ Hz), the usual equivalent circuit of a transformer, which can be seen on Fig.5, cannot be used. Although the figure shows an exact model of a transformer, it is not very useful in practical circuits and tends to be simplified.

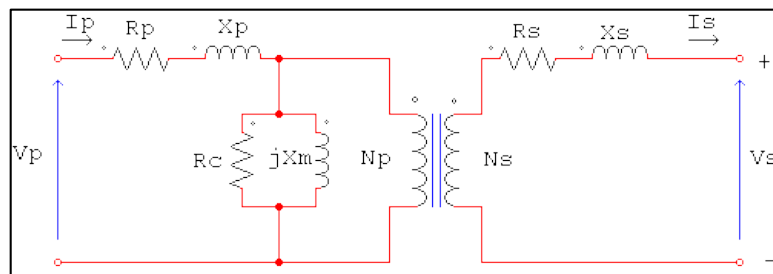


Fig. 5: Real transformer equivalent model. Source: Manual práctico de electricidad para ingenieros. Fink, Donald G.

Eventually, at such high frequencies a series of capacitances must be taken into account between the coils of the winding, between these, and between the parts of the transformer connected to ground, which at 50 Hz are totally negligible. Then, these capacities incite reactances small enough so that the currents can circulate through them.

In this way, in case that the overvoltage does not lead the system to stop, the disturbance can penetrate the transformer winding and be transmitted to the other one, causing an amplification of the wave depending on the situation. Likewise, if the oscillation of the overvoltage coincides with the resonance frequency of the system, it can be increased or transmitted to the other winding without any kind of damping.

In this field, several studies have been carried out to evaluate the effect of transient overvoltages in transformers, both by simulations using high frequency models and by using real data. An example is [11], where can be found a test carried out in 2006, and the surges transferred in distribution transformers are evaluated. In this test, a single-phase transformer without a load with a transformation ratio of 6600/690 (V/V) is used, and a voltage steep is applied directly to the transformer terminal to later measure the voltages of the LV terminal. As final conclusions, they comment that the surges transferred can be one of the main reasons for the deterioration of the transformers, since during the disturbances the voltage induced in the LV terminal is much higher during the transients. In addition, they also

demonstrate that when the nominal ratio of the transformer is low, these overvoltages can be accentuated, so it is important to consider the relationship between the inductive transferred voltage coefficient and the capacitive transferred voltage. The results obtained are reinforced by other subsequent studies, e.g. [12] [14] [15].

In [12], it can be seen a report similar to the previous one, in which some tests are again carried out using different simulations and obtaining different conclusions in this regard. Firstly, they present the most common mechanisms that can incite an overvoltage present in one of the windings of one transformer is transferred to the other:

Capacitive voltage transfer due to electrostatic induction. When the overvoltage appears in one of the windings of the transformer, as previously mentioned, the high frequencies of the perturbation cause that certain capacitances appear, despite they are completely negligible under normal conditions. In Fig. 6, the equivalent circuit of a winding is shown if the capacities appearing at high frequencies are taken into account, and the resistance of the winding is neglected. In this case L' represent the inductances of the coils of the winding, C'_d are the capacities between coils and C'_q are the capacities between the coils and ground.

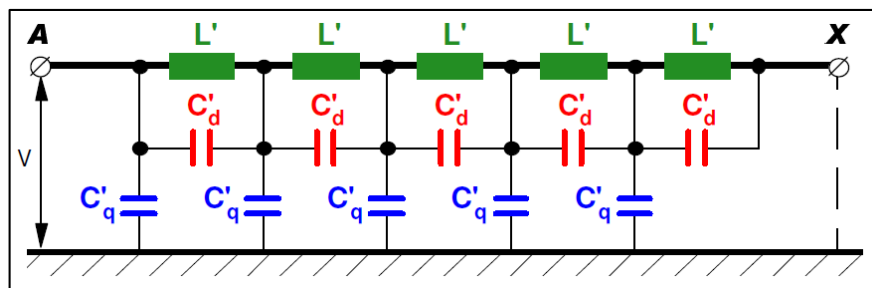


Fig. 6: Equivalent circuit of a winding of a transformer including its capacities and neglecting the resistance. Source: [10].

The values of the capacitances essentially depend on the connection of the different windings to ground and their configuration. In spite of this, not all capacitances affect in the same way to the transference of the disturbance, since for example, for the study case of [12], a large part is due to the capacitances closest to the HV winding line terminal.

Oscillatory voltage transfer (including resonance phenomena). Due to the oscillating behaviour of the transients in the windings, the transition from the capacitive to the inductive distribution causes voltage oscillations, which occur at the natural frequencies of the windings. As a result, an induced oscillation in the voltage of the secondary winding is caused, meaning possibly a considerable increase in the transferred voltage compared to what would have occurred by an electrostatic induction.

Effect of design of windings on transferred voltages. In [12], we are told about the design parameters of the transformers that can influence the impact of the transmission of surges:

- The type of windings. Apart from the capacity to ground of the windings, the longitudinal capacity of the transformer can influence the transfer of surges. In this way, the windings with a higher longitudinal capacity, e.g. interlaced or with nonloaded turns, are in better conditions due to their superior input capacity.
- Performance of windings according to the number of concentrers. Currently, there is a tendency to install for the larger transformers, a LV winding placed between two concentrers of HV windings. Then, a lower capacity of the LV winding to the ground and a greater capacity between windings is obtained, which results in higher voltages transmitted to the LV winding. Therefore, to dampen the transmission of surges it is preferable to single-concentric performance of HV winding.
- Mutual position of the winding and order of their location on the rod. The position of the windings can also influence a bit in the transmission of surges. For example, placing the low voltage winding first in the magnetic core increases the capacity of the winding in the ground, meaning advantageous in front of other configurations.
- The transformation ratio. As has been commented previously, transferred overvoltages are most dangerous for transformers with high transformation ratios.
- The connection scheme of windings and presence of grounding. When the low and medium voltage windings are connected in a triangle and one of the terminals of the line is connected to ground, or the neutral cable is connected to ground in the case of a star connection, the ground capacity of these windings increases. Therefore, through these configurations a considerable reduction in the voltage transferred to these windings can be achieved.

For the specific case of transformers in wind turbines, it is complicated to present specific data about their performance under transient overvoltages, mainly due to the lack of available bibliography. This fact is aggravated because the faults in distribution transformers are much more common worldwide, and there is also a variety of different wind turbine topologies that can vary the results. Some examples are the wind turbines that place the step-up transformer in the nacelle, that place it at the base of the tower, that place it in an adjacent housing, or inclusively there are wind turbines that generate electricity directly at

mid voltage to avoid having a step-up transformer [8]. Even so, it can be estimated that its behaviour will be similar to another one habitually used in other type of industries.

3.2.2 Generator behaviour under overvoltages

The generator to be examined in this project will be that relating to the particular asynchronous machine. This type of machine consists of a winding stator that, when injected with a three-phase alternating current, generates a rotating magnetic field; and a rotor that consists of a certain number of copper or aluminium bars, electrically connected. In this way, by means of the rotary field of the stator, a current is induced in the rotor which causes a rotatory movement until it reaches a speed close to that of the rotating magnetic field (operation as a motor). On the other hand, if an external force is applied to achieve a rotor speed higher than the relative of the magnetic field, it will begin to transfer power to the stator in the form of an electromotive force, and later converted into electricity (operation as generator).

Nowadays, the majority of the wind turbines in the world use this type of generator, also called induction generator, to produce the alternating current. In this case, this induction generator converts the mechanical energy coming from wind into electrical energy, being unusual compared to other generators connected to the grid. The main reason of this is because the generator must work with a power source that provides a very variable mechanical power. Thus, the induction motor is the one that is more adapted to these conditions to extract the maximum energy in total.

The specific type of electric machine used is the DFIG (Doubly Fed Induction Generator), which is very common for wind turbines. In this case, by power adjustable frequency AC power to the field windings, the magnetic field can be made to rotate, allowing variation in motor or generator speed. This advantage allows the generator to run at speeds slightly above or below their natural synchronous speed, being very useful because the wind speed can change suddenly. In the Fig. 7, there is a representation of the DFIG.

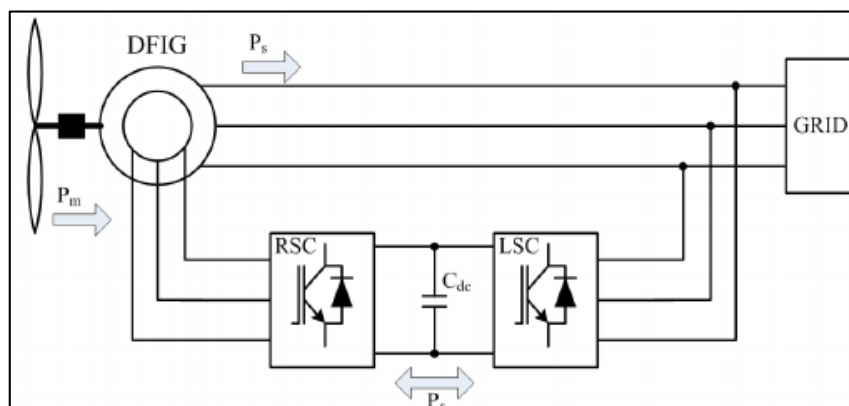


Fig. 7: DFIG scheme of a wind turbine. Source: [16]

On the other hand, as for the equivalent scheme of the generator individually, it is exactly the same as that of any induction generator. As for its standard equivalent model, it is very similar to that of a transformer as previously seen. In the following figure, it can be seen the most used representation:

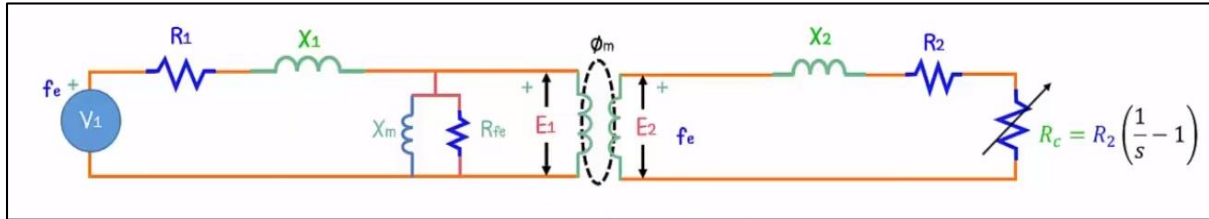


Fig. 8: Equivalent circuit of the induction machine with an electrical resistance equivalent to the mechanical load.
Source: <https://www.youtube.com/watch?v=yS4eky8JGrE>

In the present model, the stator of the machine is the same as the primary of a transformer, which has associated a resistance and a dispersion inductance to represent the losses of the winding; and another resistance and inductance in parallel to represent the losses of the motor by heating and by hysteresis in the core of the stator. As for the rotor, the resistance and reactance of the rotor winding can also be observed, although unlike the transformer, it varies with respect to the sliding of the machine and the frequency of the system. So in conclusion, it can be said that the equivalent schemes of the induction generator and the transformer are the same, at least in the parameters present in the system.

Even so, as it has been commented evaluating the standard model of the transformer, this representation cannot be applied for lightning tests, but it can be considered that the high frequency models of the induction generator and the transformer will be similar.

Regarding its behaviour in front of overvoltages, the generator, unlike the rest of the other components, is capable of producing them, although it may be due to external causes. One of the best known is Load Rejection, which occurs when a generator feeds a large load and suddenly it is switched off, provoking an increase in the generator's speed and leading into a rise in the voltage of the bus. This could mean a potential danger for the rest of the loads and for the other elements of the system. To avoid this, the generator has to reduce its voltage to equilibrate the system again and, in case the generator's speed is not supervised, an overvoltage relay is recommended. [17]

Even so, an overvoltage produced by a generator intrinsically is very rare to happen, mainly because the excitation of the current that controls the voltage is usually supervised by an automatic regulation system [17]. Then, an overvoltage of this type is usually caused by a fault in the excitation control system in case the excitation input to the alternator does not match the voltage [18].

To finish, facing the transient surges such as those produced by lightning, it can be estimated that their behaviour would be similar to that of the transformer, although with some differences. Firstly, an induction generator is more solid than a transformer due to its physical design, in addition to being oversized to withstand the variations of tension that the force of the wind can produce. In the same way, it does not have a transformation relationship that could aggravate the disturbance created, as in the case of the transformer.

Even so, due to the fact that it has a rotatory element, overvoltages in an induction generator can lead to overheating and deterioration of the whole equipment if it is constantly repeated, and, in case the overvoltage exceeds its basic insulation level, breakage and ruptures could occur.

3.2.3 Power converter behaviour under overvoltages

An AC-AC converter is a solid state electronic device that converts an alternating current (AC) signal into an alternating current (AC) signal, where the voltage and output frequency can be arbitrarily modified. In our case, the type AC-DC-AC converter, which has a DC link to perform the conversion, is considered. In the following figure, it can be seen the standard scheme of a conventional power converter:

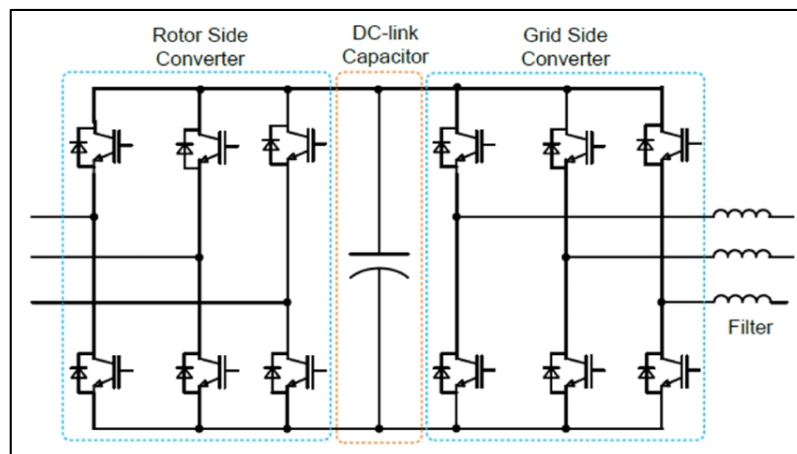


Fig. 9: AC/AC power converter scheme. Source: [19]

The composition of the presented converter consists basically of a rectifier connected to an inverter, with a direct current node with a shunt capacitor between them. In this way, a sinusoidal signal is entered through the rectifier, which is rectified by pulse-width modulation (PWM) and subsequently inverted by the same process. As for the DC link, it has the objective of storing energy so that the two conversion stages can be slightly decoupled, improving the independence and total control of the system. Even so, the capacitance occupies a large volume and considerably increases the cost of the equipment. At the same time, due to its constant use it requires a constant maintenance because of its low life expectancy.

In [20], it can be seen a report in which different tests are performed with an AC/DC/AC converter studying the voltage in each node of the equipment by varying the input voltage, which can evaluate it against disturbances. In Fig. 10, there is one of the most interesting graphs to observe the behaviour of the converter:

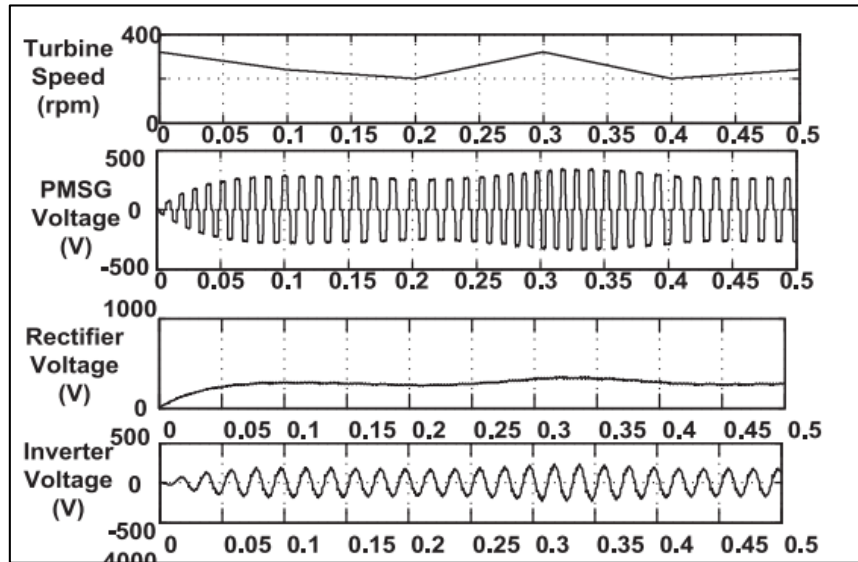


Fig. 10: Voltage behaviour in an AC/DC/AC wind turbine converter with variable wind speed. Source: [20]

In the figure, it can be seen that the converter can act as an attenuator against overvoltages of a relatively long duration, which can be beneficial for the stability of the system. Even so, the transistors generate a large amount of harmonics due to their commutation process, even reaching a Total Harmonic Distortion (THD) of 75% or more [20].

Despite that, for this project the analysis of common overvoltages is not applicable, due to the high frequencies that can achieve an overvoltage caused by a lightning strike. For this case, if the basic insulation level of the equipment is sufficient so that failures do not occur, the current flows through the converter with the configuration of the transistors that is present at the moment, so they do not have an influence especially large.

In conclusion, due to the lack of bibliography in this type of tests, it cannot be assured how is the exact behaviour of the converter in front of a pulse of such high frequencies. Theoretically, we can estimate that a small voltage drop will occur due to the equivalent resistance of the equipment, transferring the disturbance in an almost identical way to the rest of the system.

3.3 TOV protection

To conclude, the effect of the surges caused by the large currents of the lightnings, and the general functioning of the arresters in a wind farm and its limitations are briefly presented below.

As can be seen in [6], the most expensive corrective maintenance that can be found in a wind turbine is the blades reparation, so at first glance, it might seem that TOV protection becomes of secondary importance. Despite this, statistically for countries with a high lightning strike density the costs for repairs can represent a high percentage of the life cycle costing of the wind farm e.g. 22.2% in Japan [21]. Accordingly, it is important to study any method to reduce the great impact that corrective maintenance can mean.

Then, the most basic protection measures to face the TOV generally in MV lines, are through an increase of the line insulation withstand capability, the use of grounded shield wires in the lines, and the installation of surge arresters [3]. Even so, the installation of a single protection element does not guarantee the total elimination of the disturbances, but the ideal would be to install all of them for optimum protection of the system.

An example of this can be found in [22], where a grafcet representation is included to efficiently design the ground system of a specific wind turbine following a linear process. In this case, it can be verified the large number of variables to be taken into account and how long the optimal design of protections for complex electrical systems can be.

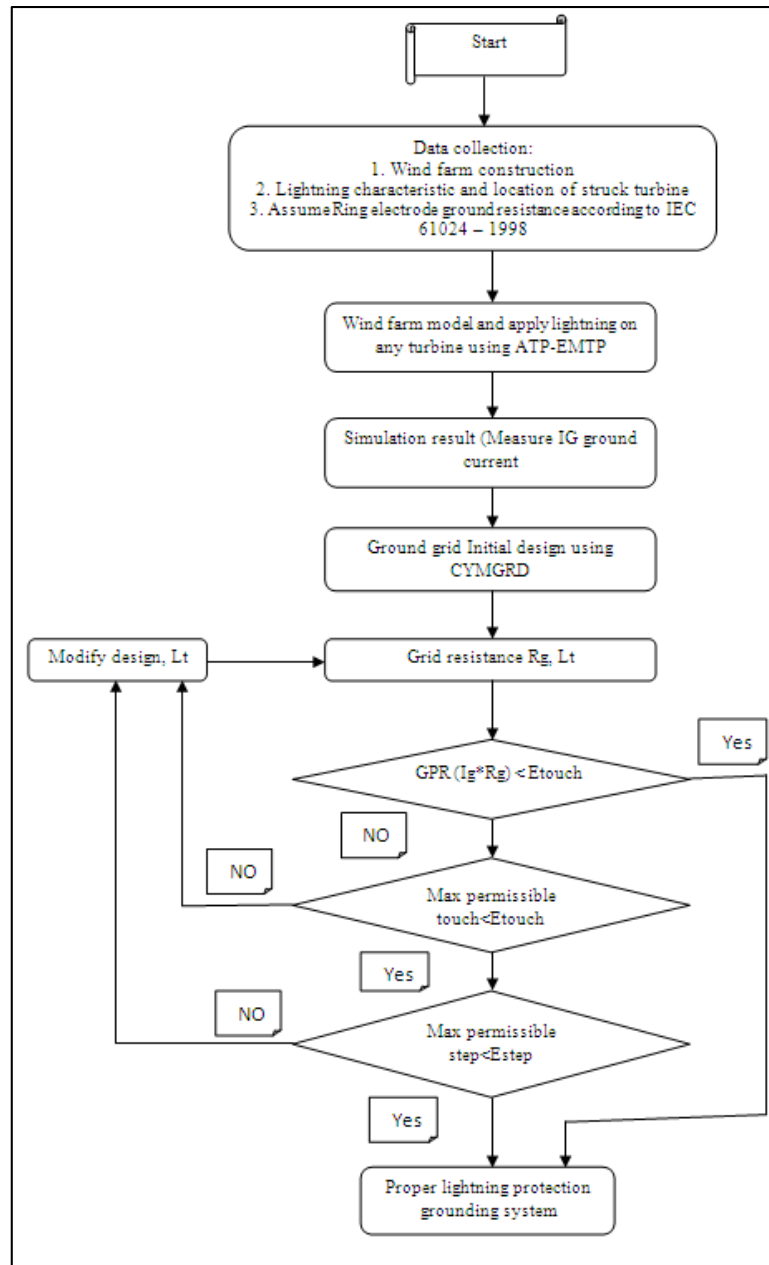


Fig. 11: Grafcet representation of a proper ground design in a wind turbine. Source: [22]

On the other hand, for the specific case of wind farms the installation of surge arresters is usually taken into account [6]. For example, according to [23], on a line of 83 km long if they are installed arises arresters every 300m, you could reduce the name of lightning outages by approximately 50%, with a reduction of about 75% for indirect impacts.



Fig. 12: Left: DEHNgard surge arrester for low voltage lines. Right: Metal oxide surge arrester for HV lines.

A surge arrester is used to protect the equipment from transients, so that it deviates the power from the overvoltage directly to ground. The main drawback of this device is its low energy density, so in case of exceeding its limit the surge arrester must be bypassed to the ground in order to avoid a breakdown [6]. In addition, as previously mentioned, there are many different configurations of wind turbines and wind farms, so it is difficult to find the optimum type, number and location of the arresters.

4. MODELLING OF THE WIND TURBINES

In this section, we will proceed to present the steps followed to obtain the models in high frequency of each of the elements of the wind turbine. To do this, an extensive bibliography of each of the elements has been reviewed to find the most functional model in simulations with lightning surges. In this way, its simplicity of implementation in the available software and its behaviour in high frequencies has been valued.

In general, it is necessary to comment that the software that will be used to implement the different models is the ATPDraw, which can limit the implementation of the most complex models. In this way, the transformer, the generator and especially the converter will be studied deeper, since the high frequency models of each can be the most complex of the entire system.

4.1 Transformer modelling

In the case of transformer modelling for high frequency surges, there is an extensive bibliography on this, mainly due to the large presence of these devices in practically all areas of industry today. Therefore, the models that could be adapted better to the project are presented in this section.

The simplest approach for this type of tests is simply by considering the capacitances that have a bigger impact on the simulation in an ideal transformer e.g. [24], [25]. In this way, although the obtaining of these capacitances is quite complicated, good approximations are achieved to frequencies of several kHz.

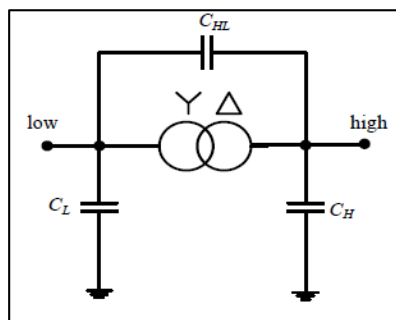


Fig. 13: MODEL 1. Ideal transformer with the most relevant capacitances. Source: [24]

The capacitors of the transformer, are represented in this case by: C_L being the capacitance of the low voltage winding to ground; C_H being the capacitance of the high-voltage winding to ground; and C_{HL} being the capacitance between the high and low voltage windings. Normally, the C_H capacitance is the lowest of all because the high voltage has more separation between the windings and between the windings and core.

Even so, to obtain more precise results it is necessary to resort to more complex methodologies to model a transformer that allows an adequate simulation of the respective high frequency tests. Therefore in [26] and [27], using the two-port theory, two very similar equivalent schemes are obtained with considerably acceptable results:

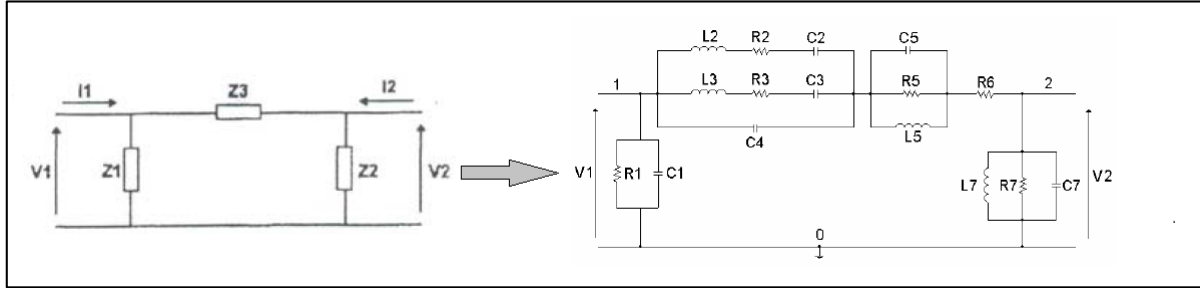


Fig. 14: MODEL 2: Two-port transformer modelling. Source: [26] and [27].

To obtain the different values that achieve the desired behaviour, a complex study has been carried out using the two-port theory. In turn, these results are simulated and compared with real tests performed in a laboratory, obtaining a very good comparison. In addition, [26] includes different values for each of the parameters depending on the power of the desired transformer. It should be noted that in [28], an extensive doctoral thesis on the modelling of transformers is carried out using similar techniques and also obtaining very valid models. In [29], using the similar approximation of Grey box transformer model to bear in mind the geometry of the transformer, it also obtains a good model adaptable to the ATPDraw software valid up to approximately 1MHz.

On the other hand, the model most used for simulations of high frequency tests in transformers is going deeper into Model 1 considering other types of effects that can influence the system. In Fig. 15 you can see an example of this type of model [30], and in [31] and [12] there are quite similar models with good results.

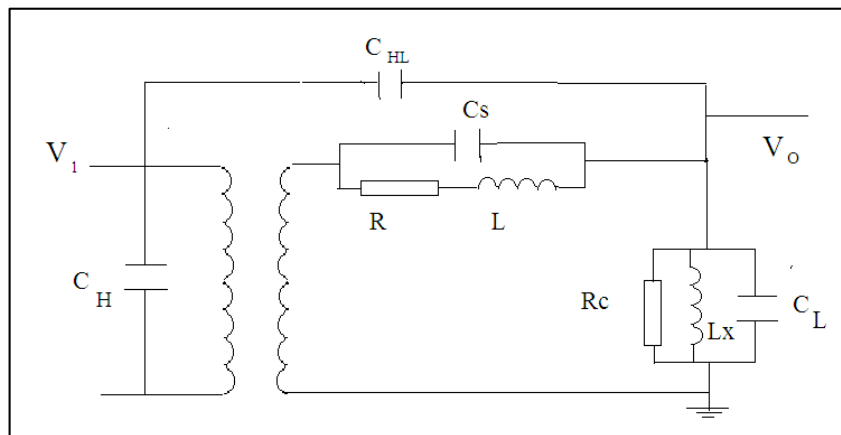


Fig. 15: MODEL 3. Single-phase transformer model for high frequencies. Source: [30]

In this case, the three-phase transformer is once again simplified into a single-phase transformer, since the perturbations propagate in a very similar way in both cases. Therefore, the model includes the impedances of the windings (R_p , R_s , L_p , L_s), the shunt elements (R_c and L_x), the same capacitances that have been discussed in Model 1, (C_{HL} , C_L and C_H), and finally the capacitance among the windings (C_s). This model has different parameters depending on the power of the transformer and has been compared with real data offering very good results.

Finally, a circuit similar to the previous one is presented [32], but this time modifying the desired parameters in order to achieve more precise results. In this case, capacitances are taken into account between the windings and between the windings and ground, the skin effects of the conductors of the windings and of the transformer core, and the resonances due to the combination of the inductances and capacitances of the windings.

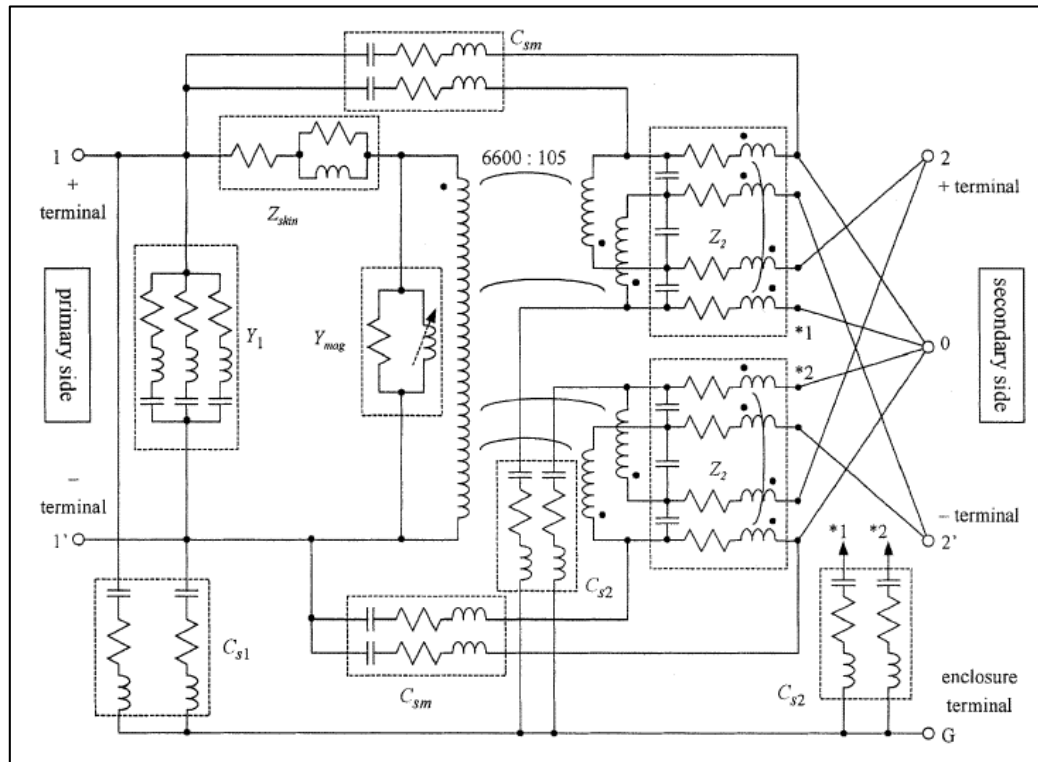


Fig. 16: MODEL 4. Core type distribution transformer model for high frequencies. Source: [32]

The parameters presented are: Winding-to-winding and winding-to-enclosure capacitance (C_{s1} , C_{s2} and C_{sm}), skin effects of winding conductors and an iron core (Z_{skin}), multiple resonance due to the combination of winding inductance and turn to-turn capacitance (Y_1 and Z_2), and saturation and hysteresis effects of an iron core (Y_{mag}). Through this model, very good results are obtained for high frequencies, but it will not be considered in the final simulations of this project because there are no specific values for the different parameters, although it should be adaptable to the ATPDraw software.

4.2 Generator modelling

For the case of the induction generator, the process to find a model for high frequencies valid for simulations with lightning is much simpler, mainly due its behaviour is very related to the transformer one. In this way as has been commented previously, the standard model of an induction generator is very similar to that of a transformer, so in short, the models for high frequencies will not be quite different.

The main difference between the equivalent models of the transformer and the induction generator is the value of its parameters, although physically they are completely differently. Therefore, in front of a lightning surge, a similar behaviour must be considered to transmit the corresponding overvoltage. Then, to obtain its corresponding representation, a model similar to that of the transformer is proposed, which is presented in [33].

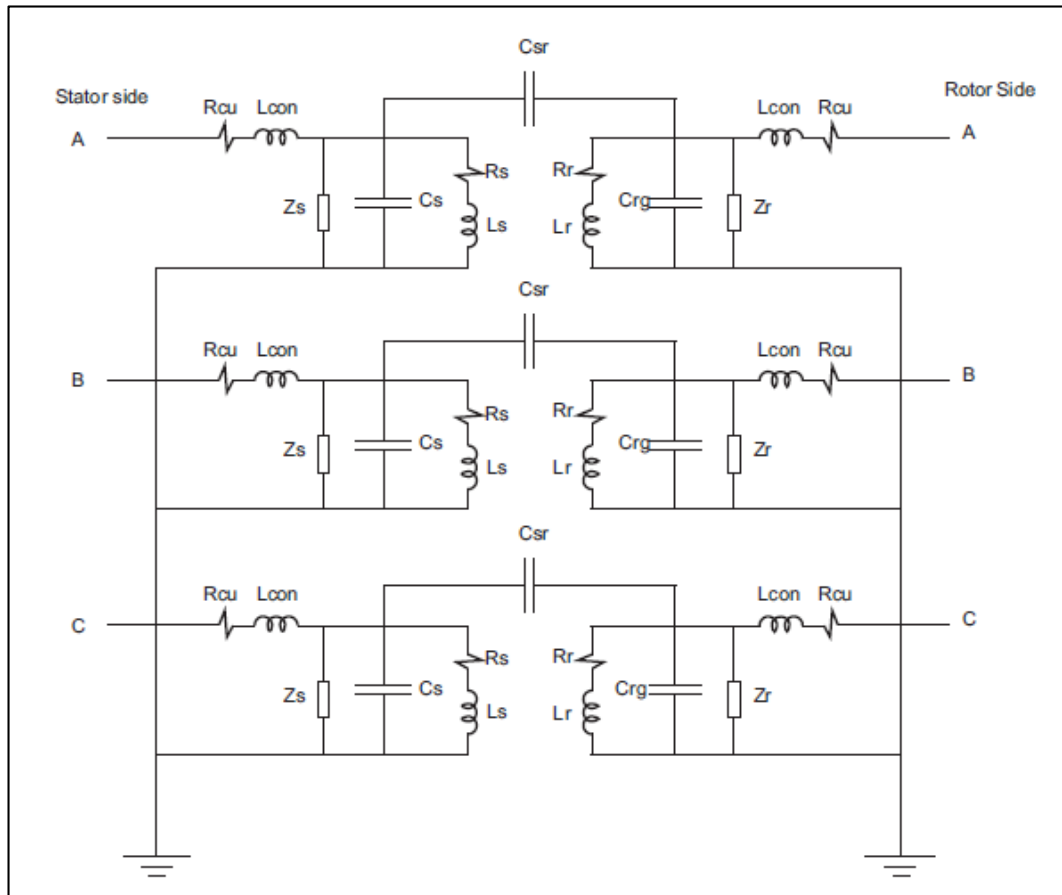


Fig. 17: MODEL 1: Three-phase induction generator model for high frequencies. Source: [33]

The presented model is very similar to the MODEL 3 of the transformer. In this case, it is the traditional scheme of the induction generator but including the capacitive coupling between DFIG stator and rotor; and the rotor inductance for a 2nd order synthesized circuit on the stator side and the capacitance between the stator and coils.

Next, the origin of the parameters presented in [33], is briefly explained.

Rcon and Lcon: These parameters represent the resistance and inductance that can appear due to the contacts and wiring of the motor.

Zs and Zr: According to [33], Zs and Zr are the impedances to reflect the attenuation in the oscillations and for integration stability of the model.

Cs and Cr: The capacitors in parallel to ground represent in this case the ground capacitance produced by the stator and rotor. Although the respective capacitances are very small, the value of the capacitance of the rotor is much lower than that of the stator.

Rs and Rr: These parameters represent the total resistance of the windings at normal temperature.

Ls and Lr: They represent an estimation of the present stator (Ls) and rotor (Lr) inductances. According to [33], the value of Lr ranges between 1/5 and 1/10 of Ls.

Csr: By last, Csr represents the capacitance that can appear in the air gap of the machine between the rotor and the stator, which is still smaller than the capacitances of the stator and rotor to ground.

Finally, in [33] different tables are collected offering some predefined values for each of the presented parameters. These values are extracted from an extensive bibliography in which they are compared explaining their origin and their significance depending on the final power of the generator in specific.

R_s [Ω]	L_s [mH]	R_r [Ω]	L_r [mH]	R_{con} [Ω]	L_{con} [μ H]	Z_s [Ω]	Z_r [Ω]	C_s [nF]	C_r [nF]	C_{sr} [nF]
0.1	30.0	0.3	5.00	0.05	1.00	500.0	1000.0	93.0	10.0	3.00

Table 1: DFIG high frequency model parameter values.

4.3 Power converter modelling

The modelling of the power converter constitutes one of the most interesting and complex parts of the present project, mainly due to the little bibliography existing in this regard. Since at the beginning of the project there was no model with proven results that demonstrated its viability for high frequencies, it was decided to follow a different path and obtain real test results in order to be able to compare them later in the proposed model. Consequently, the converter modelling process has been completely different from the rest of the parts of the wind turbine, where real data has been used and a high frequency model has been searched by other means, as will be seen in detail later.

4.3.1 Real data getting

The first step, then, was to obtain real data to compare the models that will later be considered. For this, a set of tests were carried out in a controlled laboratory to analyse the behaviour of the converter in front of high frequency impulses. In our case, as it is done in the transformers to obtain the different parameters of the equivalent circuit, we performed the open circuit and short-circuit tests. The purpose of doing these tests was to verify the comportment of the converter in both situations.

The materials used during the tests were:

- I. **Surge generator.** Its main function is to generate a brief voltage impulse to simulate a sudden front overvoltage similar to the produced by a lightning's impact.
- II. **Digital Storage Oscilloscope.** It has been used to visualize the corresponding signals and save their values for plot it later.
- III. **Amperometric clamps.** The amperometric clamps help us to measure the intensities and visualize them in the oscilloscope in a simpler way.
- IV. **BNC Cables.** They are the cables that connect the points of the system in which measure the voltage with the oscilloscope.
- V. **Banana Cables.** They are the cables that make the different connections between the elements of the system.
- VI. **Electrical power supply.** It is used in the tests to power the oscilloscope and the pulse generator.
- VII. **Grounding of Braided Copper.** In order to create a ground point with which to reference all the relevant connections, we place a physical one to ensure that there is no potential difference between them.
- VIII. **Two transistor bridges.** Inside the converter, the first of them is the responsible for receiving the alternating voltage and convert it to continuous by means of a bridge rectifier. The other, converts the DC voltage of the intermediate circuit to one of variable voltage and frequency by generating pulses.
- IX. **Capacitors.** Inside the converter, its main function is to soften the signal of the rectified voltage and reduce the emission of harmonics to the network.

In Annex I, it can be found a list of the models and a more detailed description of each of the elements. In the same way, in Annex II there are the different results obtained and the schemes for each of the tests carried out.

In the following figure, there is the set of elements presented and the corresponding connections:

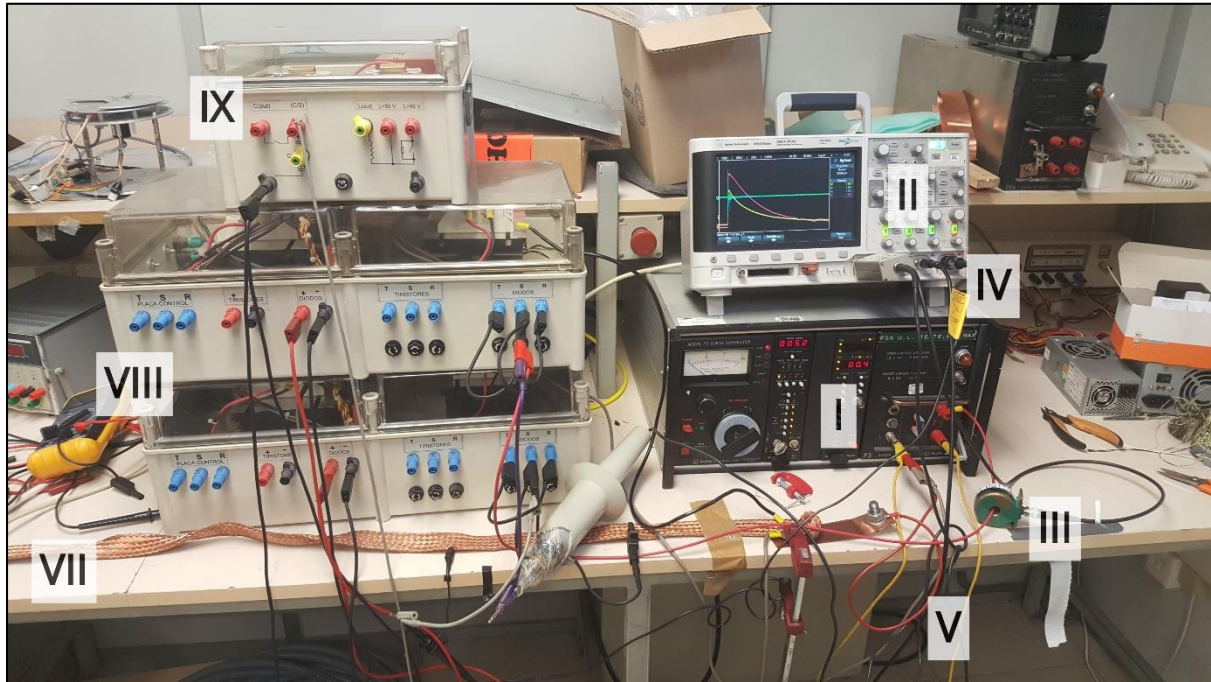


Fig. 18: Real photograph of the test carried out.

In short, it is considered that the results obtained can roughly reflect the behaviour of a simple converter against an overvoltage with a frequency and waveform similar to that produced by lightning. Then, to continue with the modelling of the converter, we will take the results obtained as good, although before, different factors should be taken into account that may result in possible variations with respect to reality:

Different amplitude. In the tests, impulses of around 400V as much were made, mainly due to the limitation of the elements of the system that we had. Even so, we must bear in mind that the overvoltage produced by a lightning could be more than 100kV, and may lead to a different behaviour of the converter depending on the possible damage, among other factors.

Variety in the waveform. Another difference that we can find in the obtained results is that the tests have been carried out with a specific impulse. In the reality, the waveforms of the overvoltage produced by a lightning strike could vary slightly, so the currents and the resulting surges could vary again.

Simplicity of the converter used. In order to study the behaviour of a standard converter, it was preferred to assemble the most basic parts that comprise it, omitting other elements that could influence in the results obtained. The main reasons for this are, on the one hand, that the configuration could present great differences from one model of wind turbine to another, and on the other, the great complexity that we

could find when studying the specific performance of the converter against overvoltages and the influence produced by the different variations. An example in this regard would be the presence of filters.

Possible imperfections in the connection during the tests. As previously mentioned, at the time of doing the tests we were limited by the material available in the laboratory. Consequently, although the tests were performed as accurately as possible, some errors can appear due to the certain imperfections in the connection of the elements or the deterioration of the measuring devices. Then, the results obtained may not be as accurate as they could be if the tests have been carried out in a more controlled environment and with more precise devices.

Test place. The geometry of the place where the converter is located may influence its behaviour in front of high frequency overvoltages. Then, the results obtained were performed in a laboratory in a controlled environment, while depending on the typology of the wind turbine, the converter can be in a completely hermetic place or at other temperatures, for example.

4.3.2 Models Review

Once obtained the practical values, the next step was to test the different models by simulations to compare the results obtained in the tests with them. But before, it was necessary to recreate through the ATPDraw software the impulse generated in them to reconstruct the laboratory conditions as best as possible.

Then, to generate an impulse similar enough to the correspondent of the physical impulse generator, it was preferred to access to its datasheet, and study its model and see how to adapt it to the software.

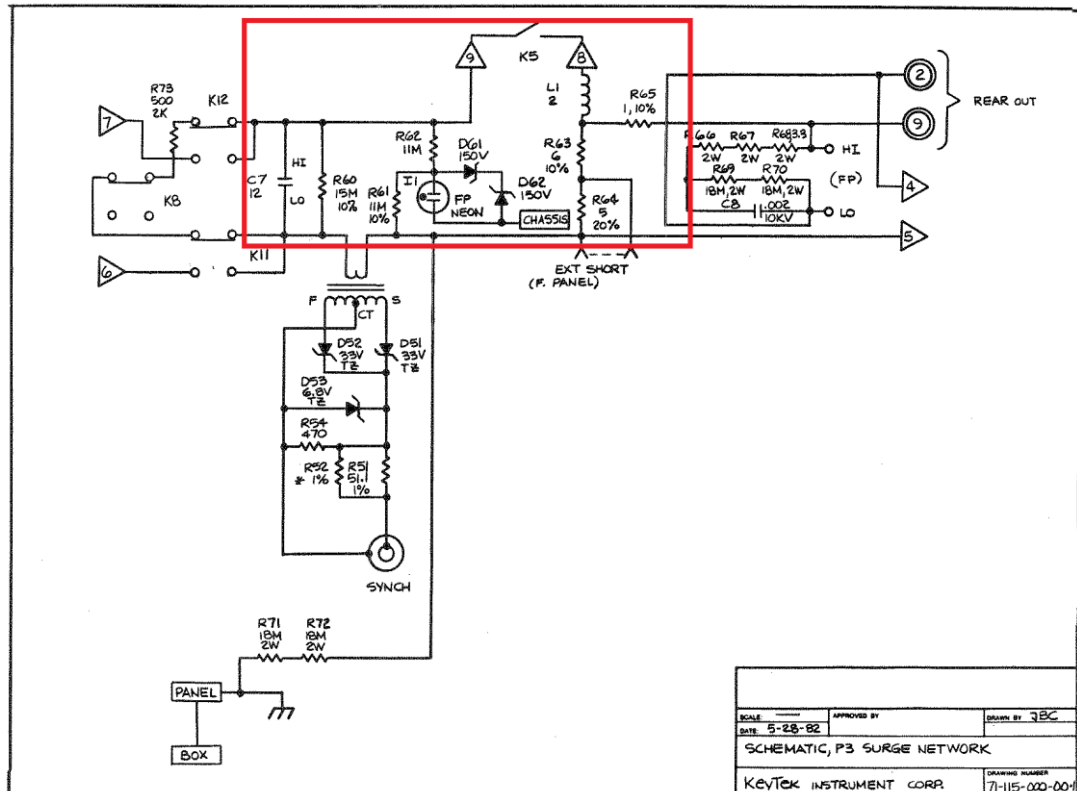


Fig. 19: Surge Network of the Surge Generator Model 711. KeyTek.

In this way, through an exhaustive study of the pulse generator model, it has been greatly simplified. The most important modifications could be the elimination of the measuring circuit, the simplification of the central resistance and the omission of the elements that do not influence the generation of the impulse. Then, Fig. 20 shows the pulse generator used to check the validity of the converter models:

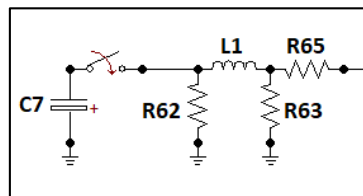
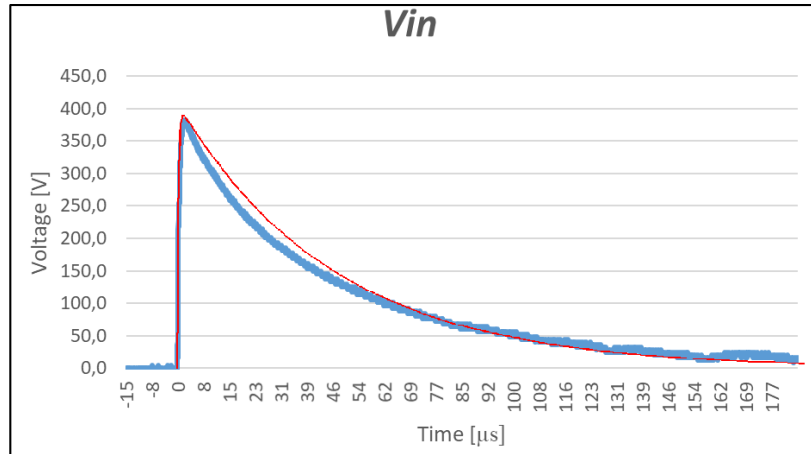


Fig. 20: Pulse generator scheme.

Into the scheme, highlight that the capacitor is at the beginning charged and, at the moment it is connected to the circuit, it discharges the pulse until it finally ends up without energy. The rest of the elements, with the exception of the R62, have a rather small influence on the voltage, but they affect considerably in the ripple and in the amplitude of the current.

Moreover, in Graphic 1 a comparison can be seen between the input voltage for the open-circuit test and the simulation of the presented pulse generator model:



Graphic 1: Comparison between the input voltage in the simulation and in the test. Red line corresponds to the ATPDraw simulation. Blue line corresponds to the Open Circuit test carried out in the laboratory.

Then, once we have the simulation of a good approximation of the impulse generated in the tests, the next step consisted on the search of a suitable model that could reflect the behaviour of the converter. First, the two-port theory was used to try to find a circuit corresponding to the voltage and current inputs and outputs of the tests.

In general, a signal is fed into one pair of terminals (input port), processed by the system, and then extracted at a second pair of terminals (output port). A two-port network is an electrical circuit with two pairs of terminals to connect to external circuits. Two terminals constitute a port if the current applied to one terminal is equal to the current emerging from the other terminal on the same port [34].

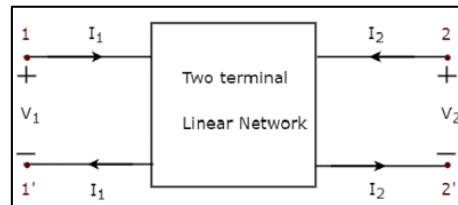


Fig. 21: Two-port network example.

Then, using the procedures that can be found in [34] and [35], the possibility of using the peak values of input and output of the voltages and currents of the obtained tests was studied, in order to find an approximate scheme of how the converter model should be.

The problem then was the great difficulty of finding a suitable model through the corresponding formulas, since the model must not only reflect the peak values of the magnitudes by the fact that the waveform is also important in this type of tests. In short, the idea of creating the model through the two-port system was rejected because of its high complexity, although it would be possible to have an idea of what the model should be like.

The first model proposed then, was the single-phase scheme of a standard converter, mainly to ensure its lack of precision at high frequencies.

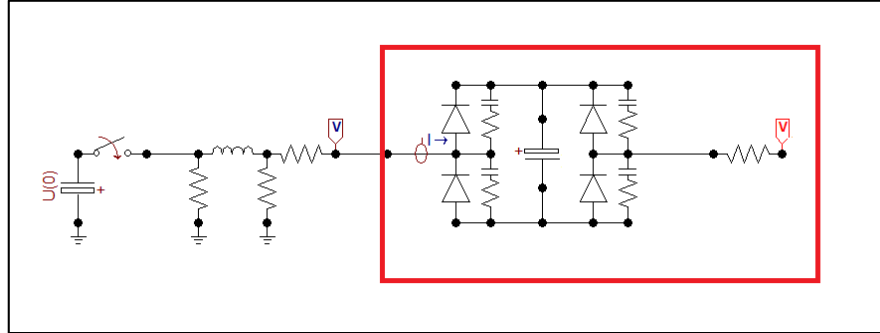


Fig. 22: MODEL 1: Standard monophasic converter model Simulation.

In this case, owing to the high frequency of the input pulse, the transistors have been simplified in their period and in an impedance parallel to it. Even so, due to the approximation that the transistors do not act for the high speed of the impulse, and for being injected only on one side, the circuit is simplified by the impedance of one of the transistors in parallel to the central capacitor.

Even so, the modest model gets a good representation of the tensions in both tests, although the problem appears in the currents of the system, which do not end up resembling the tests, so the model is discarded again.

Later, an attempt was made to evaluate the only converter model for high frequencies that is available in the bibliography presented, being the one presented by Yarú Mendez in [33]. The three-phase model presented, changes each branch of transistors by a relatively small resistance, inductance and reactance in series, with a resistance and reactance in parallel connected to ground:

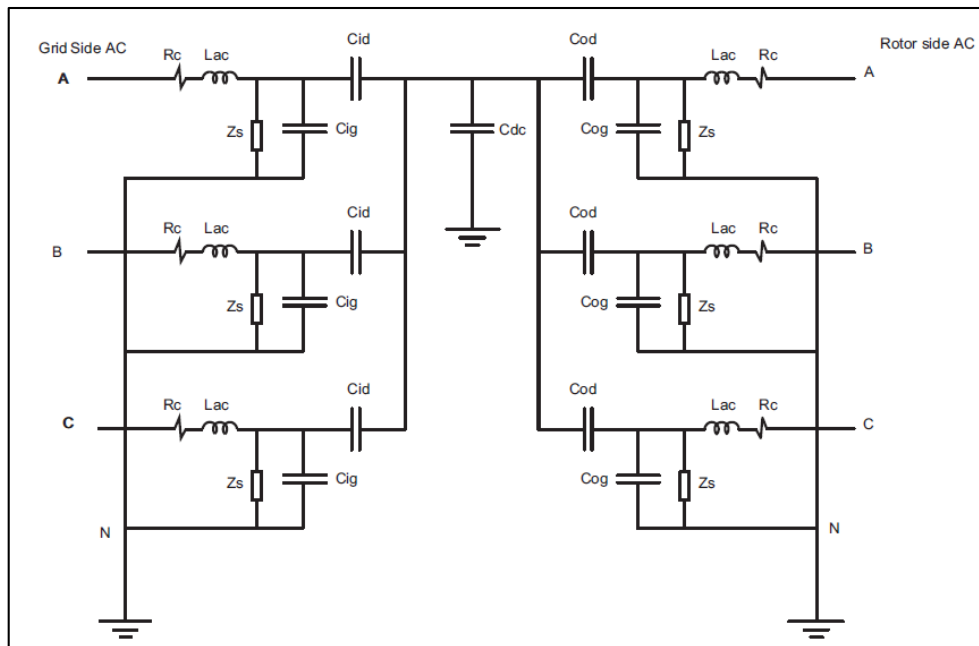


Fig. 23: MODEL 2. AC/AC converter model used for transient studies (Y-Y Connection). [33]

In the same way, in the report studied, it provides a set of values for the different parameters:

$R_C [\Omega]$	$L_{AC} [mH]$	$Z_S [\Omega]$	$C_{ig} [nF]$	$C_{id} [nF]$	$C_{og} [nF]$	$C_{dc} [nF]$
0.1	3.00	250	0.1	1.00	0.10	2400

Table 2: Values of the parameters of the converter model presented in [33].

Although many of the presented values have a logical justification, and are extensively explained in the report, we could not obtain a response similar to those of the tests performed by simulating the model in ATPDraw, not even by modifying the parameters offered. Even so, through a meticulous study of the model, certain inconsistencies in its development were observed which will be discussed later.

In brief, with the Yarú model it was not possible to reach a good approximation with the tests carried out in the laboratory. The next step then was to take advantage of the mentioned model and make a series of modifications with which to obtain the final model presented below:

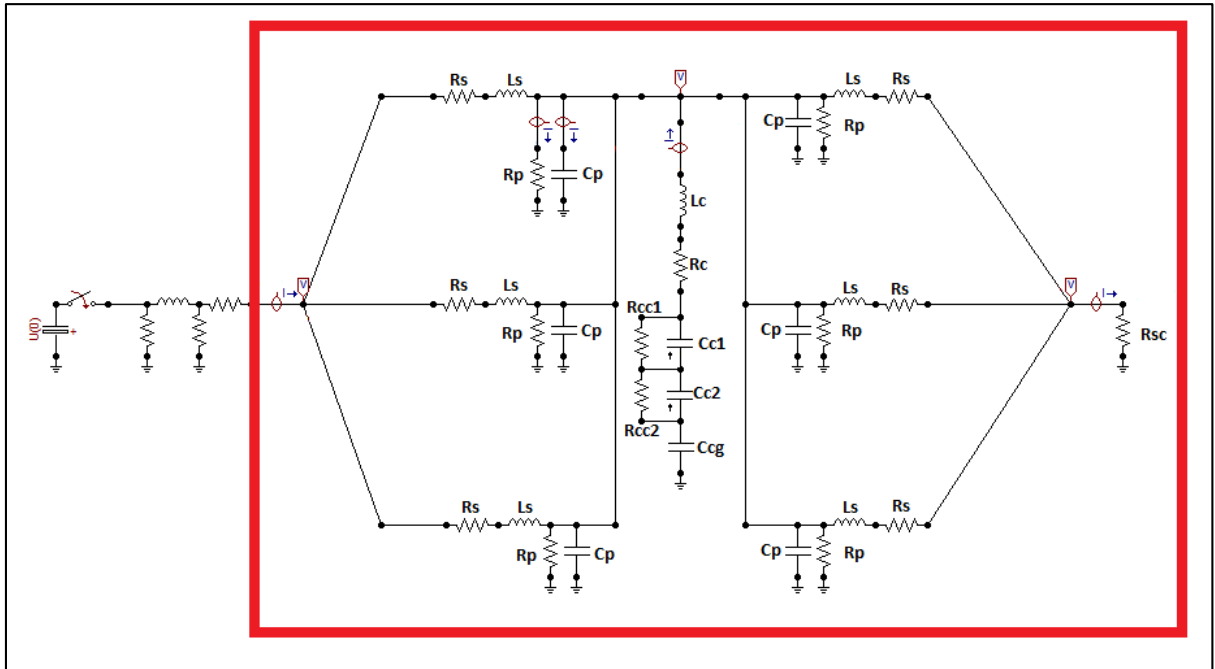


Fig. 24: MODEL 3. Final converter model scheme.

In the same way as report [33], we also provide a set of values for the parameters that achieve similar responses to those of the previously presented tests:

R_s [Ω]	L_s [μH]	R_p [$k\Omega$]	C_p [nF]	L_c [μH]	R_c [Ω]	C_{c1} [μF]	C_{c2} [μF]	R_{cc1} [$k\Omega$]	R_{cc2} [$k\Omega$]	C_{cg} [nF]	R_{sc}^* [Ω]
0.3	7.2	40	0.27	0.01	0.01	2.2	2.2	10	10	0.45	0.01

Table 3: Values of the parameters of the final converter model. *Only applies to shortcircuit test.

The values presented are estimated, which means that by a more exhaustive study, it would be possible to obtain values that allow a more precise simulation of the tests carried out. Next, a brief explanation of each of the parameters is presented, and its main difference with the Yarú model.

R_s (Series resistance). Firstly, when modelling the converter it is necessary to bear in mind the typical voltage drops in the connections and terminals. Consequently, a resistance of 0.3 ohms has been located on both sides of the inverter in each of the phases. The resulting resistance may be higher than in the Yarú model because the tests in the laboratory was not as accurate as they could have been with more precise devices.

The main influence of the series resistance in the model, on the one hand, can be reflected in the little voltage drop during the open circuit test with respect to the input voltage and the open circuit voltage. On the other hand, it has a considerable influence on the short circuit test, since the higher the resistance, the higher the input voltage and therefore, the lower the system currents.

L_s (Serie inductance). In the same way as with the series resistance, small inductances may appear in the connections and terminals, which may end up having a great impact on impulses of high frequencies such as the caused by lightning strikes. The impact on the system of these inductances can be seen in the increase in the amplitudes of the currents in both tests, and specifically during the open circuit test it is one of the main causes of the oscillations produced.

R_p (Parallel resistance). The parallel resistance in this case represents the resistance between the transistor and ground. In this case, with a resistance of 40 $k\Omega$, it is sufficient to verify its low impact on the system, although it is possible that in a real model the resistance is much higher.

C_p (Parallel capacitance). The capacitors to ground represent in this case the ground capacitance produced by the commercial low voltage circuit boards with power electronics, such as IGBTs with gel based isolating material and corresponding drive circuits [33]. These capacitances can also be a reflection of the ground capacitance caused by the diodes.

The effect of this capacitance at high frequencies can be seen actively in the open circuit test, since it has a great influence on the amplitude and on the wavefront of the current of the whole system. As for its value, an approximation can be made by looking at model 2.

Lc and Rc (Central resistance and inductance). In the same way that Rs and Ls, at the time of realizing the model it has been thought that it could be interesting to take into account the voltage drop and the small inductance of the connections and terminals of the DC bus. The impact it has on the system is very low, and it can be appreciated on how small the values of both magnitudes are.

Cc1 and Cc2 (Central Capacitors). The modelling of these capacitors is really intuitive, since they are physically located in the DC bus of the converter. Then, by simply checking the data of the capacitors in their datasheet an exact value of the actual system has been achieved. The value of the capacitor mainly affects the amplitude and wavefront of the currents.

Rcc1 and Rcc2 (Resistances of the central capacitors). Although the present resistors do not have a direct impact on the magnitudes of the presented model, the DC bus capacitor's datasheet physically locates them in parallel of each capacitor, so it has been decided to place them in the same place to offer more realism to the final model.

Ccg (Capacitance to ground of the central capacitor). The most important change made with respect to model 2, is the situation of this capacitor between the central capacitor and the ground. The reason for the appearance of this capacitance, it is believed to be the same as in the case of the Cp, but instead of being due to the transistors and diodes that are switched on, is for those that do not act at the moment of the surge.

The greatest impact of this capacitance is very similar to that of the capacitance in parallel, since they have a very similar origin. In short, the amplitude and waveform of currents vary considerably depending on the value of the capacitance, which can be similar to the Yarú model again [33].

Rsc (Short-circuit resistance). Finally, the ground resistance in the short circuit test is presented. The origin is similar to that of the series resistance, since it is again due to voltage drops in the connection. Therefore, it is thought that both its value and its magnitude are quite similar to those of the series resistors.

4.3.3 Main improvements of model 2 to obtain 3

In this section, it can be seen which have been the most important modifications made to the Yarú model [33] to obtain a behaviour of the system in front of a surge similar to those of the tests presented.

Starting with the modifications that have the most impact on the model, it is necessary to highlight the capacitance C_{cg} firstly. Previously, it had been thought not to locate any element in the terminal of the central capacitors, since in the real systems they are in floating configuration. Even so, studying the Model 1 meticulously and the origin of capacitances C_p of the Model 2, we saw very logical to locate the capacitance C_{cg} as it is in Model 3, achieving a response much more similar to the tests carried out than before.

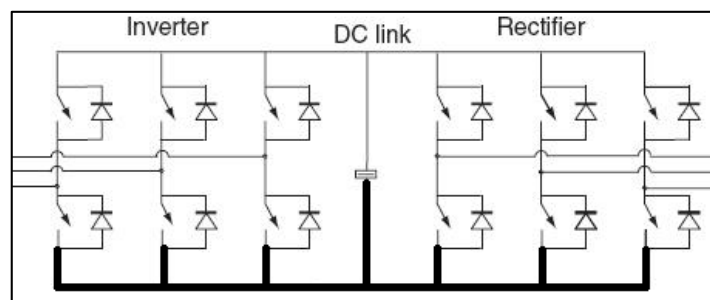


Fig. 25: Real connection of an AC/AC three-phase converter.

Another important modification is the representation of the transistors, although the capacitance C_p has been maintained. On the one hand, the capacitances in series C_{id} and C_{od} of Model 2 have been suppressed, since they have not been found a physical justification for their existence and, in addition, they amplified the amplitude of the currents and made them much slower, which intensifies the difference between the model and the real data. On the other hand, the value of the parallel resistance has been increased, since the resistance to ground cannot be only 250 ohms.

Finally, although it does not have a great impact on the behaviour of the model, an attempt has been made to convert the central capacity into a model closer to reality. In this way, the resistance and inductance of the wiring and terminals have been included and the actual configuration of the central capacitor has been simulated, consisting of two capacitors of 2.2 μF in parallel with two 10 $\text{k}\Omega$ resistors.

4.4 Other elements of the wind turbine.

For a correct development of the rest of the parts of the wind turbines, it has been used as a reference the essays [8], [36], [37], [38], [33], [39], [7] and [40]. In them, different simulations are carried out in order to study the behaviour of the different elements against transient overvoltages. In addition, the results are compared with real measurements to verify the accuracy of the study.

In order to perform the pertinent simulations valid, they must include specific models of each element that composes the wind farm, and that can have a direct impact on the study of surges. Despite this, as we have seen previously, there is no specific model for each component and may vary depending on the study [33]. Therefore, for each element, the most realistic and suitable model for the study of high-frequency overvoltages caused by both direct and indirect lightning impacts will be selected.

Rotor blades

Among all the bibliography reviewed for the present project, a multitude of different models have been found to electrically represent the blades of the wind turbine, since as it has been commented, there is no specific model accepted by the regulation. Next, the most appropriate ones are presented to simulate the behaviour of the blades against overvoltages, choosing the most adequate for the study considering the limitations of the ATP software.

Firstly, the approximations that are included in [39] and [37] are presented. In them, the path to ground is represented approaching as a line of transmission without losses. The consideration of all three rotor blades (not coupled by field between each other) is important for accurate estimation of reflection behaviour at the hub. In this way, they are treated as a conductive cylinder, adapting to the following equation:

$$Z_{blade} = 60 \ln \left(\frac{2H}{Rc} \right) [Ohm] \quad (1)$$

Being: Z_{blades} : Equivalent impedance of the blades.
H: Height of the cylinder.
Rc: Base radius.

Although the model presented is not completely invalid, the geometric approximation is quite incorrect, so the model presented in [33] can be considered more accurate. Its model is based on a principle similar to the previous one, and its proper formula is the following:

$$Z_{blade} = 30 \ln \left(2 \frac{(h_{blade}^2 + r_{blade}^2)}{r_{blade}^2} \right) [Ohm] \quad (2)$$

Being: Z_{blade} : Equivalent impedance of the blade.
 h_{blade} : Equivalent mean-height of the blade.
 r_{blade} : Equivalent radius of the segment of the rotor blade.

This time, each blade of the wind turbine is divided into three different sections, so that the result is geometrically more similar to the real one. However, frequency-dependence of the blades as well as lightning surge attenuation on the blades is not accounted for in these simple models, mainly because they are represented as simple constant-value and distributed-parameter transmission lines [8].

Thus, in [38], it is presented another frequency independent transmission line model, the Constant Parameter (CP). The frequency dependence of the parameters is not considered again, leaning this time on [40], in which the authors concluded that the transient response of the system can be neglected and the skin effect has a little influence on the lightning transient response. The CP line model basic equations are:

$$\frac{dV(x,t)}{dx} = -R'I(x,t) - L'\frac{dI(x,t)}{dt} \quad (3)$$

$$\frac{dI(x,t)}{dx} = -G'V(x,t) - C'\frac{dV(x,t)}{dt} \quad (4)$$

The CP line parameters have to be calculated using the technical information of the wind turbine, e.g. material characteristics and dimensions of components. In the same way as the following model, the CP line model can be used to represent the tower and the blades.

On the other hand, in [7], a method is presented by which the structure is simplified as a multiconductor grid in the shape of cylinder. It is built in frequency-domain to take into account the effect of the frequency-dependent characteristic of the resistances and inductances on lightning transients. As the model is based on the wind turbine towers, although it is applicable to the blades, it is described in detail below in the section of the tower.

Finally, in [8] we are told about the existence of a model for extra high voltage (EHV) transmission line towers, which include frequency-dependence and surge attenuation. However, sophisticated models of complete wind turbines are needed, composed with very detailed experimental measurements of scale models.

Bearings

The fact of modelling the rotor blades, main and yaw or azimuth bearings of the wind turbine is usually omitted in the vast majority of the projects found in this regard. The reason for this can be found in [33], where they are modelled as a series resistance to an inductance, using the Finite Element Program (FEM). The results obtained in the test using real data show resistances of the order of 10^{-5} Ohms, and 10^{-4} μ H, so they can be neglected without practically changing the final result of the simulation.

Tower

Regarding the modelling of the tower, in some of the bibliography reviewed the model of the blades and the model of the tower is calculated in the same way for their geometry similarity. Then, the [37], [38], [33] and [39] models presented previously in the section of the blades can be applied too for represent the towers. The model of [7] can be used to represent both, but it is quite different because it is more oriented to characterise the tower.

Thus in [7], as mentioned above the tower body is simplified as a multiconductor grid in the shape of cylinder, where a set of analytic formulas are deduced for evaluating the circuit parameters of the branches in the multiconductor grid. The hybrid equation is built in the frequency-domain, and then the discrete Fourier transform with exponential sampling is used to obtain the lightning transient responses in different parts of the tower body. The main drawback with this method is that through simpler ones, good results are achieved, without the need to resort to complex numerical systems and the appropriate software.

In the same way, in [41], [42] and [43] there are models for high frequencies for transmission line towers. In this area there are a lot of different models, since the issue of lightning strikes in transmission lines is very common throughout the world. It can be seen the typical equivalent impedance model in [41] and a very interesting model of equivalence of the tower modelled as a network of cylindrical wires in [43]. Even so, it is worth highlighting report [42], which presents different models and compare their responses.

In conclusion, the model finally chosen is the correspondent of the equivalent impedance as in [37], taking profit of the ATPDraw distributed transposed line model. The main advantages of this model are its simplicity, its ease at the time of implementing it in the available software and its accuracy when evaluating the high frequency tests.

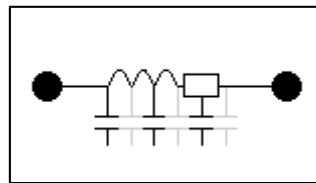


Fig. 26: ATPDraw distributed transposed line model (Clarke).

Power cable system

In the case of the modelling of the power cable system, there is an extensive bibliography on this matter, due to the fact that lightning strikes are very common in distribution lines. The most simplified model that can be found is by an equivalent impedance, since as the size of the line is relatively small, it is a good approximation e.g. [24], [44]. Logically, the equivalent impedance must take into account many technical factors such as the geometry of the cable, its configuration, the size of the insulation, etc.

Even so, taking advantage of the fact that the project is being carried out using the ATPDraw, there are different usable elements of easy implementation that can result in a better approximation than a simple equivalent impedance. Therefore, as in [45], [46] and [47], the LCC tool will be used:

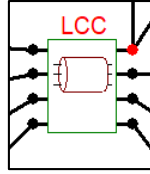


Fig. 27: ATPDraw LCC model.

The present element allows to simulate among a great variety of types of lines with great precision, providing in addition the option of choosing the equivalent model desired by the user. For our case, we take advantage of the Enclosing pipe system and the PI model, since we do not need to adapt exactly one model specifically.

Ground-termination system.

The correct design of a ground system, as seen in the TOV Protection section, can be an arduous task, especially if environmental and technical conditions, as well as economic and statistical ones, are valued. Even so, for a precise modelling of the system, it is not necessary to employ complicated mathematical processes, since as will be seen below, by placing simple elements considerable accuracy is achieved.

The most widespread model, when making simulations is through a fixed resistance, of around 5 or 10 ohms in total. An example can be found in [48], where a study of the ground system of a wind turbine is made simply by different values of a fixed resistance adding a small inductance. In addition in [33], taking advantage of the formula developed in [49], using the resistivity of the soil, an approximate size of the electrode and its depth, it obtains a fairly accurate value of its grounding:

$$R' = \frac{\rho}{\alpha \cdot 2\pi^2 \cdot rc} \cdot \ln \frac{\beta \cdot 8rc}{\sqrt{2ad}} \quad (5)$$

In the same way, even for the evaluation of transients produced by lightning, in [50] it is commented that the modelling of the ground system by a fixed resistance is sufficient, although the equivalent impedance should be found to have a transient characteristic which converges to a grounding steady state value.

On the other hand, we can find the study carried out in [24], which highlights the difference in behaviour of the ground system during the lightning due to the very high frequencies of the electric impulse. When making a good design, it is important to take this factor into account, since the surges produced can deteriorate the different elements of the system.

$$R_t = \frac{R_0}{\sqrt{1 + \frac{i}{I_g}}} \quad (6)$$

Being: R_t : Equivalent impedance of the ground system.

R_0 : Equivalent impedance of the ground system in standard conditions.

i : Current through the rod (kA).

i_g : Critical current for soil ionization.

The problem at the time of applying the system is the fact that the currents vary with time, so it cannot be implemented using the available software.

In the same way, it is necessary to mention that there are different studies that try to compensate the non-linearity of the ground system through a set of inductances and conductances conveniently located. Some examples can be found in [51], [52] and [47], where they offer some formulas depending on the parameters and the related equivalent schemes.

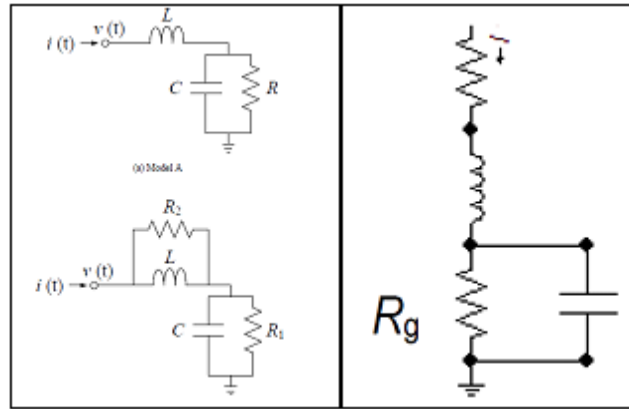


Fig. 28: Examples of high-frequency models for ground systems. Sources: Left: [52]. Right: [47].

Finally, the High-frequency segmented RLC circuit method is presented, which will be implemented in the final simulation. In this case, the electrode is divided into N fictitious segments to take into account the non-uniform distributions of the charge and current, and each segment of the electrode is represented by an RLC section [53]. In the Fig. 29, a scheme about the RLC Segmented Ground Model is presented:

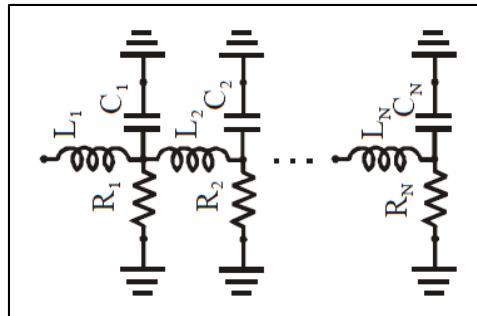


Fig. 29: Segmented RLC Ground model. Source: [54]

The respective equations to obtain the different parameters are:

$$R_n = \frac{\rho N}{2\pi l} \cdot \ln \frac{2l}{a} [\text{Ohm}] \quad (7)$$

$$C_n = \frac{2\pi\epsilon l}{N} \cdot \left[\ln \frac{2l}{a} \right]^{-1} [Farad] \quad (8)$$

$$L_n = \frac{\mu_0 l}{2\pi N} \cdot \ln \frac{2l}{a} [Henry] \quad (9)$$

Being: ρ : Resistivity of the ground.
 ϵ : Permittivity.
 l : Total length of the ground system.
 N : Number of segments.
 a : Radius of the ground cable.

Comparing the results from all the models, the segmented circuit achieves the best performance during lightning strokes simulations, being hardly exact until 1MHz. The exception can be found in extremely conductive soil with a resistivity of 10 $\Omega \cdot m$ or less.

5. FINAL RESULTS

In this section the basic configuration chosen for the wind turbine with which to make the final simulations will be presented. Subsequently, the data chosen for the different parameters of the program will be justified, while a brief description of each one is offered. Finally, the different simulations will be carried out and the behaviour of each element will be interpreted in front of the perturbations, evaluating if the final model is adapted to the initial objectives of the project or not.

5.1 Wind farm characteristics

Regarding the characteristics of the wind farm, since this project does not try to simulate a specific real case, a set of approximate values of what would be a medium-power wind turbine will be used. For this, the external geometrical characteristics of the system, the geometry of the wiring and the power of the most characteristic elements of the turbine will be presented.

First, the following figure shows the configuration of the wind turbine to be simulated later:

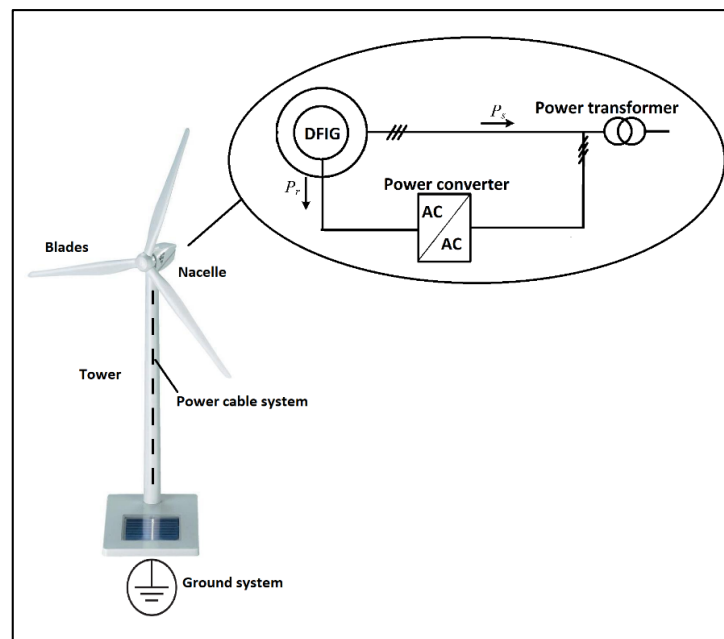


Fig. 30: Simplified scheme of the wind turbine to simulate.

Logically, the scheme represents a very simplified version of a wind turbine. Even so, it has been decided to consider these elements because they are the most representative of the system and they are the most relevant at the time of transferring the impulse produced by a lightning stroke. In addition, in previous sections it has been commented that wind turbines can have a large number of topologies and different configurations, but by not simulating a specific real case, the most installed one nowadays has been chosen.

To continue, a table with the parameters mentioned for the different parts of the wind turbine is presented:

Equipment	Parameter	Unit	Chosen value
Blade	Length	Meter	50.0
	Radius	Meter	0.004
Tower	Length	Meter	80.0
	Radius of the base	Meter	1.50
Power Cable System	Tower length	Meter	80.0
	Distance between wind turbines	Meter	300.0
Transformer	Rated power	MW	5.0
	Transformation ratio	NA	20/0.69 kV
Generator	Rated power	MW	3.60
Ground system	Resistivity	Ohm*meter	750

Table 4: Geometry and Power of the main elements of the wind turbine.

Again, as we do not try to represent a case of wind turbine in particular, we have preferred to present approximate values for each element, in the convenience of the study. In this way, although some of the parameters are not entirely coherent, as the objective of the study is to observe the behaviour of the system under the perturbations of a lightning strike, the results are perfectly valid.

The geometrical parameters of the nacelle have not been included since it has not been necessary to calculate its equivalent scheme, because only a practically negligible resistance will be used. As for the power converter, for having obtained a new model without an extensive comparison of its performance against disturbances, it is not possible to specify its power, although it could be estimated.

5.2 Simulation tools

In this section, we will explain in detail the ATPDraw tools with which certain specific parts of the wind turbine have been simulated, since the program has specific elements for this. In the same way, the values chosen for each of the parameters that are necessary will be justified and, in case the chosen data come from another report or are estimated, it will also be indicated.

5.2.1 Lightning current source simulation

To achieve an accurate simulation of the lightning perturbation, it is important to bear in mind all the parameters related to it and introduce them to ATPDraw correctly. In this case, the software presents a tool for these type of signals specifically, named HEIDLER Current Source, which is adapted to generate the desired current or voltage signal depending on the necessities of the user. The software has other similar tools to introduce a current impulse with the characteristics of a lightning, but the input data of the HEIDLER type is more similar to the presented previously, being so more intuitive.

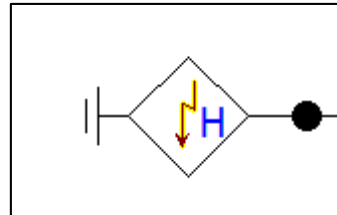


Fig. 31: Heidler Current Source from ATPDraw Software.

Regarding its viability, the HEIDLER Current Source is used for lightning simulations in multiple studies using the ATPDraw software, e.g. [32], [25] and [47]. Then, a Table with the parameters to introduce, its unit, a brief description of each and the final chosen value is presented below:

	Unit	Chosen value	Description
Amplitude	Ampere	30000	Defines the peak value desired for the impulse.
T_f	Seconds	$1.2 \cdot 10^{-6}$	Defines the front duration of the impulse. It is the interval of time between the beginning of the impulse until its peak value.
Tau	Seconds	$50 \cdot 10^{-6}$	Defines the stroke duration. It is the interval of time between the beginning of the impulse until the point on the tail where the function amplitude has fallen to 37% of its peak value.
n	NA	2	It is a factor which influences the rate of rise of the function. In other words, if n is increased the maximum steepness increases too.
T start	Seconds	0	Defines the instant of time when the current impulse starts.
T stop	Seconds	1000	Defines the instant of time when the impulse has to finish.

Table 5: Parameters of the HEIDLER Current Source.

To find some realistic values for the different parameters, they are chosen to achieve a current wave shape of $1.2/50 \mu\text{s}$ and a current amplitude of 30 kA, which will occur in a wind turbine with a probability of 50% [32]. With respect to the T stop value, a predefined value of 1000 seconds is established, representing that the impulse will continue without a limit until it stops by itself.

As a final comment, the current source will be located in the peak point of a blade, mainly because the majority of the lightning strokes will happen in this place. Despite this, there are cases of lightning strokes in nacelles, and in the same way its effect will be considered on another wind turbine of the same wind farm in the final simulations section.

5.2.2 Blades and tower simulation

In the case of the blades and the tower, the ATPDraw tool for distributed transposed lines will be used, as mentioned before in the modelling section. Again, we will take advantage of equation (1) to obtain the value of the necessary parameters required by the program to perform the simulation.

Actually, the mentioned tool is conventionally used to simulate transposed lines of several phases within the program. The case is that as it allows to take into account the set of resistances, inductances, capacitances and conductances that can appear in this type of circumstances, the monophasic line type is used to make a very good approximation. Next, a table with the most important parameters is presented:

	Unit	Blade chosen value	Tower chosen value	Description
R/I	$\frac{\text{Ohm}}{\text{meter}}$	0	0	Define the present losses by Joule effect on the line for each meter.
Z	Ohm	607.0	200.0	Defines the Modal surge impedance of the line. It is defined by $Z = \sqrt{\frac{L'}{C'}}$, taking in account the total length of the line.
v	$\frac{\text{meter}}{\text{second}}$	190·106	255·106	Defines the Modal propagation velocity. It is defined by $v = \frac{1}{\sqrt{L' \cdot C'}}$.
Length	meter	50	80	Defines the total length of the line.
Conductance	Siemens	0	0	Defines the conductance of the line. In the case of relatively short lines, they are usually underestimated, but can be calculated using $G=R \cdot C'/L'$.

Table 6: Parameters of the transposed distributed line tool.

At the time of choosing the parameters, it has approached the blades and the tower as their metallic parts without Joule effect losses, since they would not have a great impact in front of the final results. Likewise, the conductance of the system has been underestimated due to the short length of both elements. On the other hand, seeing the Modal propagation velocity of the conductor, the formulas present in [55] has been used. For this, in the rotor blades a relative permeability of 2.5 has been used due to the presence of insulating materials, and in the tower an 85% of the tower's speed has been imposed, being somewhat superior to the previous one.

Regarding their situation in the system, the blade rotor will be right next to the Heidler Current Source, since this is where the lightning usually impacts. Then, the tower is connected to the rotor blade and, at the time, it is connected to the ground system. Between both elements the nacelle equipment will be connected, mainly due to they are physically located in that place specifically.

5.2.3 Power cable system

For the simulation of the wiring, the LCC tool will be used for line testing of the ATPDraw software, as mentioned in the modelling section. First, it is important to emphasize that the power cable system is divided into two distinct parts, and it is on the one hand the wiring from the nacelle of a wind turbine to the base of the tower, and on the other the wiring present between two wind turbines.

At that time, the LCC tool that is used requires a large number of parameters that must be included to obtain an accurate simulation, and in our case for not having a specific case, it has been necessary to estimate some of them. In addition, it is essential to take into account both the core and the sheath of the cables, so the great precision of this tool can be emphasized for the simulation of cables and conductors.

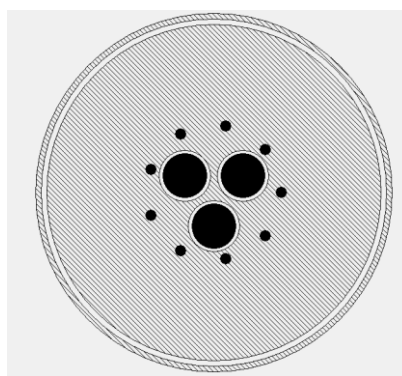


Fig. 32: LCC Cable representation.

In the Figure, the configuration approach for the LCC tool is presented, both for the wiring of the tower and for the wiring between wind turbines. Then, the Figure consist on two types of cables; on the one hand the three-phase cable remain in the middle of the cable system, with a bigger size than the other nine conductors and surrounded by a sheath layer. On the

other, nine small conductors, which are connected in both ends to ground, are located adjacent the others to represent in a better way the behaviour of the system in front of a lightning perturbation. In other words, the three main cables are presented to extract the energy from the generator and are surrounded by the equivalent of a conductive envelope to be able to consider the currents induced in the system.

In the following table, there are the different parameters of the power cable system. It should be borne in mind that the only difference between the cable of the tower and the one that connects the wind turbines between them is the length, being 80 and 300 meters respectively.

	Unit	Three-phase cable values		Coverage	Description
		Core	Sheath		
Rho	Ohm* meter	$2.3 \cdot 10^{-6}$	107	$2.3 \cdot 10^{-8}$	Defines the resistivity of the conductor material.
Freg. Init	Hz	50	50	50	Defines the frequency at which the line parameters will be calculated, or the lower frequency point of parameter fitting, depending on the model.
Rin	Meter	0	0.02	0	Defines the inner radius of the conductor.
Rout	Meter	0.02	0.023	0.005	Defines the outer radius of the conductor.
Mu	NA	1	1	1	Defines the relative permeability of the conductor material.
Mu (ins)	NA	1	1	1	Defines the relative permeability of the insulating material outside the conductor.
Eps (ins)	NA	2.7	2.4	4	Defines the relative permittivity of the insulating material outside the conductor.

Table 7: Parameters of the LCC tool.

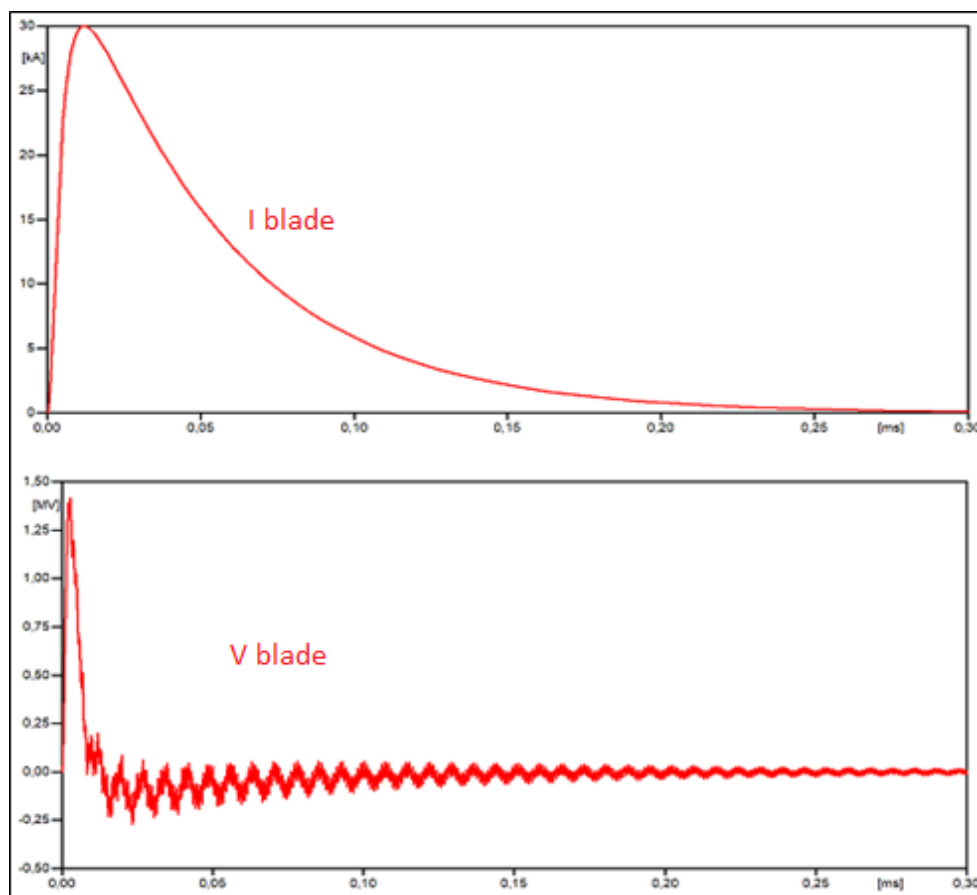
The parameters that stand out in this case are the resistivity and the radius of the conductors and insulators. For the resistivity, a value somewhat higher than copper has been selected, to take into account the high temperatures and the conditions of a cable in a wind turbine; and for the insulation of the three-phase cable a value similar to that of plastic material has been chosen. Regarding the size of the electrical conductors, a radius of 20 mm has been chosen for the three-phase cable (1256 mm^2), and 5 mm for the coverage (78 mm^2). It is necessary to emphasize that they are not simulations of a specific case of wind turbine, so it is possible that the data is not as accurate as it could be in physical facilities.

5.3 Wind turbine Simulation

Once all the models of the different components of the wind turbine and the tools to be used by the ATPDraw are presented, the results obtained in the final simulations and their validity will be analysed below. Then, the final model to be simulated in the available software is presented by sections in the Annex IV, due to the large size it reaches for all elements to be taken into account.

Then, we will proceed to study the behaviour of the whole system through the waveforms and amplitudes of voltage drops and currents that circulate throughout the system as a result of the application of the lightning stroke. Consequently, it should be considered that the parts that can have the greatest impact on the project will be deepened, and the parts that may be more trivial will be summarized.

Firstly, the graphs that are obtained as a result of reviewing the lightning strike in the blade of the wind turbine are presented:



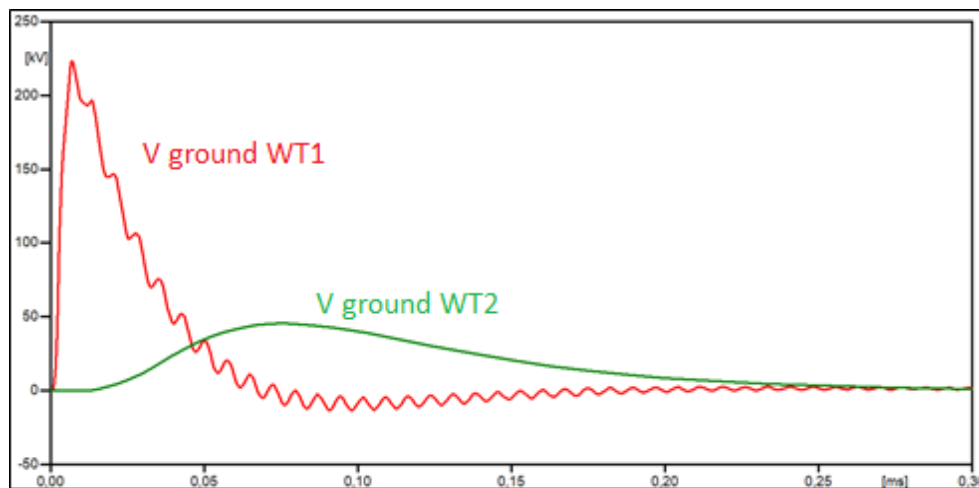
Graphic 2: Waveform of the voltage at the point of the lightning stroke (down), and the waveform of the current flowing through the blade towards the nacelle and the tower (up).

In the figure, it can be seen that the lightning stroke in the blade produces an overvoltage of 1.41 MV in approximately 2.65 microseconds and a current of approximately 30 kA. The

values of both parameters are the typical ones that can appear in these cases, being a current so high that could damage the equipment of the system, including the most robust parts such as the blades or the nacelle.

As additional comments, it is worth noting the great distortion that can be seen in the voltage waveform, which may be due to different resonances of the capacitances and inductances of the electronic equipment of the system. In addition, it should be noted that in the simulations the ground system implemented has been used as a reference instead of the ideal ground, since in this way a much more realistic simulation of the behaviour of the entire wind turbine is achieved.

Consequently, since we are not simulating an ideal ground system, it can be seen in Graphic 3, as there is an overvoltage of 223 kV in the system of the first wind turbine:



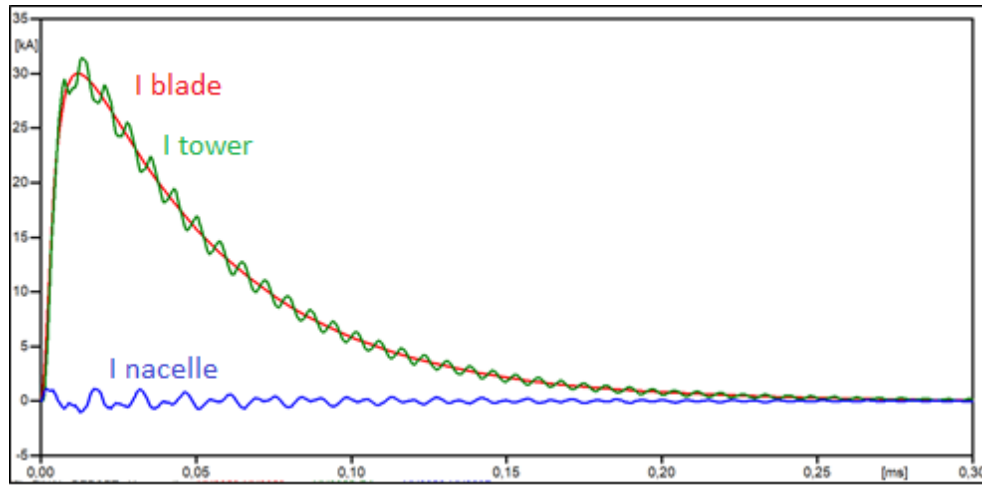
Graphic 3: Voltage Waveform of the Ground System. Red line: Ground WT 1. Green line: Ground WT 2.

Although it may seem a very large overvoltage for a ground system, it must be taken into account that a ground resistivity of 700 ohm·m has been selected, which is relatively high. In addition, the overvoltage practically disappears in less than 0,5 ms. Even so, this voltage peak in the ground system could lead to upward currents and damage some equipment that may not have been directly affected by the lightning strike.

Moreover, in the same figure it can be seen how a much smaller overvoltage (45.5 kV) appears in the ground system of another wind turbine. This phenomenon can be caused by the transmission of the disturbance through the wiring between turbines and through the ground system. In other words, even if a wind turbine is not directly affected by a lightning strike, if the protection system is not adequate, faults could occur to the wiring and to the different equipment due to the overvoltage of the ground system.

Next, the effects of the transferred disturbances to the devices of the nacelle will be commented. Firstly, in the Graphic 4 there are evidences that despite the majority of the

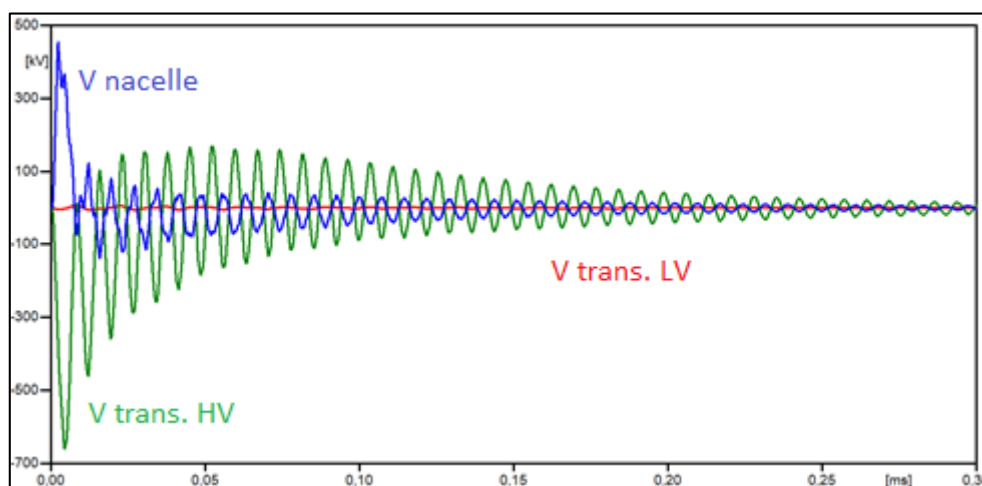
current is deviated to the ground system through the tower, a part is transferred to the nacelle ($I_{\text{peak}} = 1140 \text{ A}$) and consequently, to the equipment which is inside it.



Graphic 4: Current through the blade (Red line). Current through the tower to ground (Green line). Residual current that is transferred to the nacelle (Blue line).

In this case, even if we are in a favourable situation due to the connection to ground, for the high lightning currents a small part that must be considered is transferred to the nacelle, meaning a potential risk for the equipment. At this level, the overvoltage produced in the nacelle reaches a peak of 453 kV.

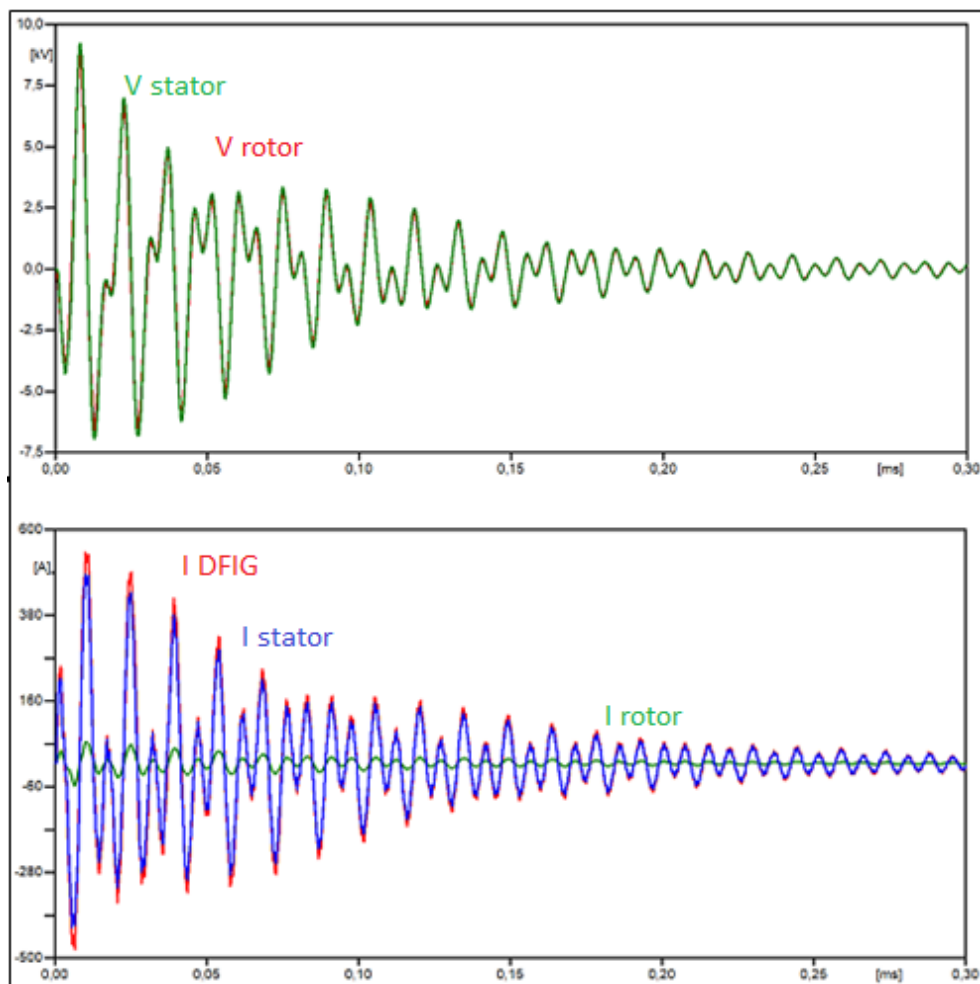
Then, this overvoltage that appears in the nacelle, for being in contact with the equipment, equals its potential causing an anomalous behaviour of all of them. An example can be seen in the transformer, where a voltage of around 8800 V appears in the primary, but, due surely to its transformation ratio and to its connection, a peak of 659 kV is reached in the secondary. The waveform of the voltages can be seen in Graphic 5:



Graphic 5: Voltage at the Nacelle (Blue line). Voltage at the primary of the transformer respect to the nacelle (Red line). Voltage at the secondary of the transformer respect to the nacelle (Green line).

As explained above, the transformer behaves in a way that causes an increase in the overvoltage that appears in the primary, meaning a greater danger to the power cable system located on the secondary, which is analysed below. For the transformer voltage measures, it is necessary to bear in mind that they are referenced to the nacelle, since it is where the ground physical connection is made and brings a higher accuracy to the simulation.

Next, connected to the primary of the transformer is the DFIG, composed by the power converter and the induction generator. The configuration of these equipment, as previously seen, is based on the connection of the output of the converter and the stator of the generator to the primary of the transformer, and the rotor of the generator to the input of the converter. Therefore, the following figure shows the amplitudes and waveforms of currents and voltages in the DFIG:



Graphic 6: UP: Voltage at the Stator of the Generator (Green line). Voltage at the Rotor of the Generator (Red line). DOWN: Current transferred to the DFIG system (Red line). Current transferred to the Stator of the generator (Blue line). Current transferred to the rotor of the generator (Green line).

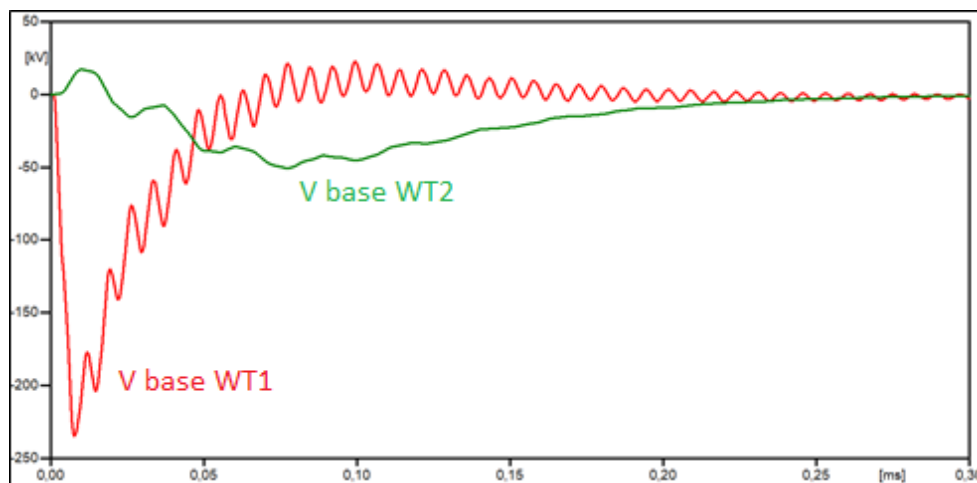
Regarding the graph, first of all, it should be noted the small impact referring to the overvoltage produced, since both the rotor of the generator and the stator have a very

similar voltage. Even so, although the graph cannot reflect it, between both points there is a voltage drop of almost 500 V, probably due to the effect of the power converter or the transmission of the induction generator. The shape of these voltages perfectly reflects the real tests performed to evaluate the behaviour of the power converter against the disturbances produced by lightning strikes.

For these overvoltages that are present in the generator, in the power converter and in the transformer, is where the possibility of damages in the equipment must be taken into account. To consider this factor, as previously mentioned, it is necessary to study if the peaks of the surges obtained are bigger than the basic insulation level of each equipment, and then evaluate whether they have been affected by the disturbance or not. Depending on the result, the placement of surge arresters in the system should be considered.

As for the currents of the graph, it is verified that the large amount of current flows to the generator stator, probably because the modelled power converter can be of a lower power than would correspond in this type of installation. In spite of this, the behaviour of the converter again reflects the one seen in the real tests. In short, it can be seen how the majority of the current is deviated to ground through the typical total winding resistances of the model of the induction generator.

Finally, the last graph to be examined is that of the overvoltages at the base of the wind turbines, which logically will be very similar to that of both ground systems:



Graphic 7: Voltage at the power cable system at the base of the tower of WT1 (Red line). Voltage at the power cable system at the base of the tower of WT2 (Green line).

For this case, either due to the wiring between both wind turbines or to the ground system, at the base of the adjacent wind turbine to which the lightning has fallen, the overvoltage that can be seen is produced. As a result, an overvoltage of approximately 50 kV peak could be transferred to the elements of the second wind turbine, even though it has not directly suffered a lightning strike.

5.3.1 Evaluation of the overvoltages including a surge arrester

Once the behaviour of the models has been evaluated, the results are complemented with a simulation of the system including a surge arrester located on the high voltage side of the transformer. For this purpose, the MOV tool of the ATPDraw software will be used, by placing three surge arresters in the three-phase line.

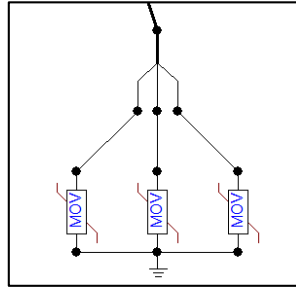
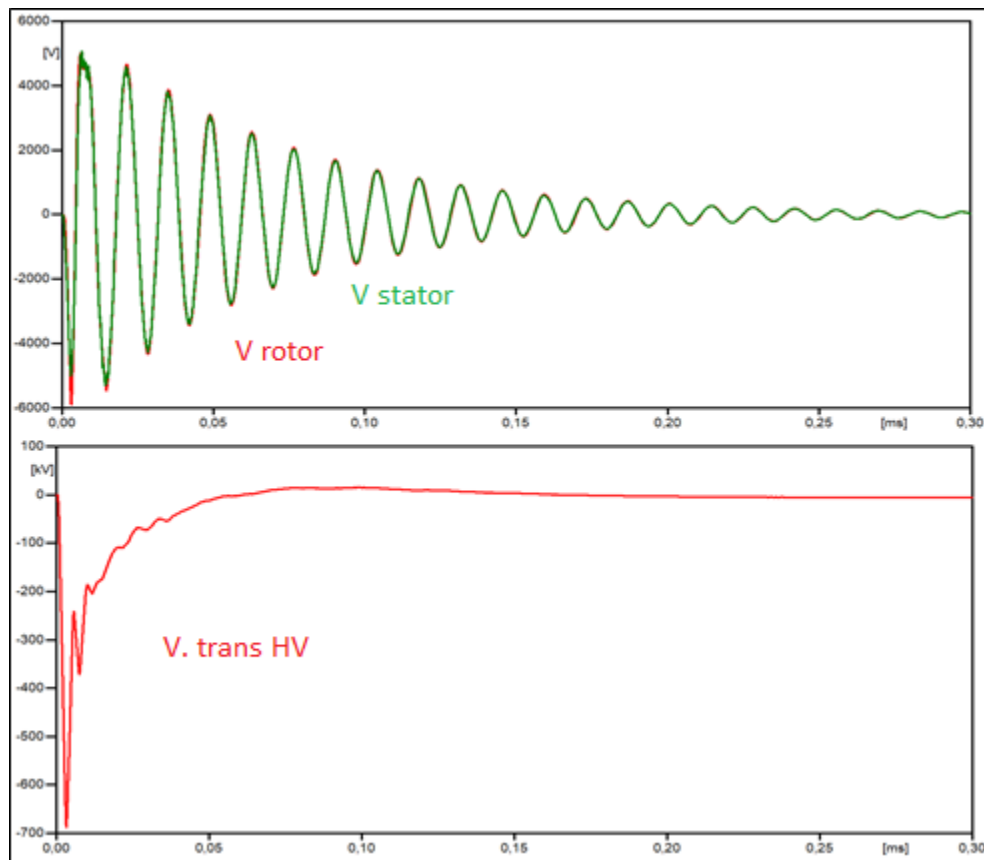


Fig. 33: Surge arrester configuration of the final simulation.

The reason for using three single line surge arresters instead of a three phase one, is only to offer more clarity to the simulation and make it more intuitive. Next, the overvoltages will be presented in the most susceptible equipment of the system, to evaluate the protection offered by the surge arresters in the face of a lightning strike with respect to a traditional system.



Graphic 8: UP: Voltage at the Stator of the Generator (Green line). Voltage at the Rotor of the Generator (Red line). DOWN: Voltage at the HV side of the transformer.

If we compare the actual overvoltages in the stator and in the rotor with the respective ones in graphic 6, it can be seen that in both cases, the peak of the overvoltages has been reduced by around 40% of the total. In this way, depending on the BIL of the equipment, a more than remarkable protection of the equipment against the lightning strikes has been achieved.

As for the overvoltage produced in the secondary of the transformer, it can be seen how the maximum peak remains the same as in figure 5, but also the disturbance is extinguished much earlier. As a result, the energy capacity is greatly reduced, offering great protection to the entire system.

Finally, although some arresters have been placed with a reference voltage of 18 kV in the secondary of the transformer, it is necessary to say that by means of a more intensive study on the placement and type of the arrester, an even greater protection could be achieved in comparison with the presented one. Even so, as has been mentioned previously, surge arresters present a set of disadvantages and, if the economic variable were considered, the problem would be even more complex than the current one.

5.4 Limitations and possible improvements of the project

The following is a list of certain limitations that have had to be considered at the time of carrying out the project:

Possible changes in the equipment studied in a wind turbine. As can be observed, many of the references used throughout the project consist of tests to obtain the high frequency model of a specific element of the system. Even so, depending on the situation of each on the wind turbine, its behaviour could vary slightly with respect to the tests in a controlled laboratory.

Possible changes in the configuration of the wind turbine. Although the typical scheme of a conventional wind turbine does not usually vary depending on the model, it is possible that different electronic components are included as a filter, for example. It could modify the behaviour of the system against the disturbance caused by a lightning strike.

Perform more accurate tests for the converter. As we have seen previously, the test carried out in the power converter in the laboratory to study its model presents a follow-up of specified limitations, as mentioned in the modelling section. In this way, by means of specific tests of a conventional wind turbine converter, more accurate data could be obtained to model it.

Use more complex software. If instead of the ATPDraw software, another program was used to include another models consisting of more complex numerical methods, much more accurate results could be obtained for other types of studies.

With the purpose of improving the current project, we propose a follow-up of possible improvements to deepen the subject and obtain other conclusions in this regard:

Improvement of the models applied. First, as a main improvement, it is proposed to use a better software in which include more complex models of each element than previously presented. In this way it could be possible get more accuracy at the time of evaluating the behaviour of the wind turbine.

Add more wind turbines to the system. By introducing other wind turbines, it would be possible to evaluate the effect of lightning strikes on a wind farm seen from a more global point of view.

Evaluate a specific wind turbine. One possibility to obtain more solid results would be through the introduction of specific parameters in the different elements of a real model. In this case, so many estimations would not be necessary and it would be possible to evaluate the system in a much more realistic way.

Include protection measures. Another way to expand the project would be by placing different protective equipment and studying its effectiveness depending on the type chosen and the place of its location.

Perform an economic study. To complement the previous improvement, it would be possible to carry out a study depending on the geographical situation of the wind farm to assess its risk of suffering some type of damage due to a lightning strike. Therefore, the costs of the protection equipment must be evaluated depending on the area to estimate the economic viability of the project as opposed to the corrective maintenance of the systems.

Evaluate the future IEC CDV 61400-27-1. By the end of this year 2018, The International Electrotechnical Commission (IEC), which is a worldwide organization for standardization comprising all national electrotechnical committees, will propose a new law to specify the standard dynamic electrical simulation models for wind turbines and wind power plants.

The main object of IEC is to promote international co-operation on all questions concerning standardization in the electrical and electronic fields, so the new law intends to specify some wind turbine models to be used in wind power plants models or to simulate wind turbines without wind power plant relationships.

6. CONCLUSIONS

In the present project the transient energy characteristics of a wind turbine under natural lightning has been investigated through proper modelling and simulation. To do this, the most suitable high frequency models for each element have been studied, without using a specific wind turbine model. At the end, the results of the final simulations obtained are included, with which the proposed models are validated and checked.

As a result, it could be considered that it has been possible obtain a model of wind turbine suitable for tests in which evaluate its behaviour against the disturbances produced by a lightning strike. So, although there are certain limitations in the accuracy of the final results, the models have been compiled and analysed as appropriate as possible for each element, bearing in mind the predetermined objectives at the beginning of the project and the complexity of the system.

In this way, observing the final simulations, it is possible to interpret that the different elements behave in a way that could be expected, since they correspond to what logically should be obtained. Even so, to achieve more solid conclusions, a more exhaustive study of the load flows of the system would be necessary, comparing them at all times with data obtained from cases of real lightning strikes in wind turbines, monitoring it with the appropriate measurement equipment.

Regarding the specific power converter, it has been possible to obtain a model to represent high frequencies, motivated mainly by the absence of this type of studies. To do this, different models have been considered and, specifically, the one presented in [33], which has been modified to achieve the expected behaviour.

In fact, it could be assured that the power converter model has a very similar operation to the one that the equipment would have in the reality during a disturbance with a waveform similar to the one produced by a lightning strike, as can be seen in the annexes and in the final simulations. For this, many factors that are normally neglected have had to be taken into account by estimating their parameters and evaluating them. Consequently, to find a response more similar to a real case, it would be necessary obtain data from a converter with the adequate power to be installed in a wind turbine, and study it against the disturbance corresponding to a lightning strike.

In short, as a final conclusion it can be highlighted that the initial objectives have been satisfactorily achieved, obtaining a wind turbine model considerably suitable for lightning simulations; developing a new model of a power converter for high frequencies that can offer very good results; and a set of possible improvements to the present project that could become very interesting for the world of wind energy.

7. BIBLIOGRAPHY

- [1] "Asociación Empresarial Eólica (AEE)," February 2018. [Online]. Available: <https://www.aeeolica.org/>.
- [2] J. M. Ponce, "Global Energy," 07 November 2017. [Online]. Available: www.globalenergy.com. [Accessed 01 March 2018].
- [3] A. Piantini, "Lightning Transients in MV Power Distribution Lines," V Russian Conference on Lightning Protection, São Paulo, 2016.
- [4] D. Robinson, "Storm Highway," [Online]. Available: <http://stormhighway.com>. [Accessed 02 03 2018].
- [5] E. (. E. d. Galicia), "Ega (Asociación Eólica de Galicia)," 12 01 2009. [Online]. Available: <http://www.interempresas.net>.
- [6] M. Ishii and J. Montanyá, "Renewable Energy Systems - Wind Power Systems".
- [7] X. Zhang and Y. Zhang, *Calculation of Lightning Transient Responses on Wind Turbine Towers*, Beijing: Hindawi Publishing Corporation, 2013.
- [8] P. Sarajcev and R. Goic, "A Review of Current Issues in State-of-Art of Wind Farm Overvoltage Protection," *energies*, 2011.
- [9] H. Odoglu, *BEST Transformer Tests*, Balikesir: Balikesir Elektromekanik Sanayi Tesisleri A.S, 2009.
- [10] M. Á. R. Pozueta, *Sobretensiones en los transformadores*, Cantabria: Universidad de Cantabria, 2010.
- [11] M. Popov, L. v. d. Sluis and R. Smeets, *Evaluation of surge-transferred overvoltages in distribution transformers*, Holland: ELSEVIER, 2006.
- [12] Federal State Unitary Enterprise All-Russian Electrotechnical Institute, "Transferred Overvoltage on Nonloaded Transformer Windings: Evaluation of Voltage and Protective Measures," *Elektrotehnika*, Moscow, 2015.
- [13] Merlín Gerín, *El transformador y su entorno, para una protección máxima*.
- [14] M. Florkowski, M. Kuniewski, J. Furgal and P. Pajak, "Investigation of Overvoltages in Distribution Transformers," *IEEE*, Kraków, 2017.
- [15] J. Das, S. MIEE and PE, "Surges transferred through transformers," *IEEE*, Atlanta, 2002.
- [16] Ş. Demirbaş and S. Bayhan, "Grid synchronization of doubly fed induction generator in wind power systems," in *International Conference on Power Engineering, Energy and Electrical Drives*, Torremolinos, 2011.
- [17] "All kinds of faults in an alternator and their protection.," *Electrical Engineering Blog*, 10 October 2012. [Online]. Available: <http://eblogbd.com/faults-in-an-alternator/>.
- [18] Electrotechnik, "Types of faults in an alternator," March 2014. [Online]. Available: <https://www.electrotechnik.net/2014/03/types-of-faults-in-alternator.html>. [Accessed 02 August 2018].
- [19] M. Ebeed, "Enhancement Protection and Operation of The Doubly Fed Induction Generator During Grid Fault," 2013.
- [20] N. Singh and V. Agarwal, "Single-stage AC-AC power conversion for WECS," Allahabad, 2013.
- [21] E. Mizuno, "Overview of wind energy policy and development in Japan.," in *Renewable and Sustainable Energy Reviews*, 2014, pp. 999-1018.
- [22] M. N. A. A. S. M. A. Abd-Allah, "A Proper Design of Wind Turbine Grounding Systems under Lightning," in *World Academy of Science, Engineering and Technology*

International Journal of Electrical and Computer Engineering., 2014.

- [23] S. P. d. Silva, A. Piantini, J. L. D. Franco and J. Gonçalves, "Lightning performance studies for a 13.8kV distribution network," in *7th International Symposium on Lightning Protection (SIPDA)*, Sao Paulo, 2003.
- [24] M. A. Abd-Allah, M. N and A. S. Ali, "Towards an Accurate Modeling of Frequency-dependent Wind Farm," in *WSEAS TRANSACTIONS on POWER SYSTEMS*, 2014.
- [25] M. A. Abd-Allah, A. Said and M. N. Ali, "Mitigation of Lightning Hazards at the More Sensitive Points in Wind Farms Using Ant-Colony Optimization Technique.," in *Journal of Electrical Engineering*, Shoubra.
- [26] A. Piantini and A. G. Kanashiro, "A distribution transformer model for calculating transferred voltages.," Sao Paulo.
- [27] A. G. Kanashiro, A. Piantini and G. F. Burani, "A methodology for transformer modelling concerning high frequency surges," VI International Symposium on Lighting Protection, Santos - Brazil, 2001.
- [28] K. Imdad, "High Frequency Modeling of Power Transformers under Transients," 2017.
- [29] B. Jurisic, I. Uglesic, A. Xemard and F. Paladian, "High frequency transformer model derived from limited information," in *Electrical Power and Energy Systems*, 2017.
- [30] M. Fernando and V. Cooray, "Lightning Surges at Distribution Transformer Secondary," in *International Conference on Industrial and Information Systems*, 2010.
- [31] W. Wijayapala, J. Lucas and L. Hasthanayake, "A Methodology to Develop a Distribution Transformer Model for Transient Studies," in *ENGINEER - Vol. XLIX, No. 02*, Sri Lanka, 2016, pp. 51-59.
- [32] R. Rodrigues, V. Mendes and J. Catalão, "Lightning Surges on Wind Power Systems: Study of Electromagnetic Transients.".
- [33] Y. Hernández, T. Tsovilis, F. Asimakopoulou, Z. Politis, W. Barton and M. M. Lozano, "A simulation approach on rotor blade electrostatic charging and its effect on the lightning overvoltages in wind parks.," Venezuela, 2016.
- [34] J. O. Attia, "Two-Port Networks," in *Electronics and Circuit Analysis using MATLAB*, CRC Press LLC, 1999.
- [35] S. P. S. N. Rishabh Verma, "Brief study of two port network and its parameters.," in *INTERNATONAL JOURNAL OF INNOVATIVE RESEARCH IN TECHNOLOGY*, 2014.
- [36] B. Badrzadeh, M. H. Zamastil and E. Isabegovic, "Transients in Wind Power Plants—Part I: Modeling Methodology and Validation," in *IEEE Transactions on industry applications*, IEEE, 2012, pp. 794-806.
- [37] J. Birkel, E. Schulzhenko, J. Kolb and M. Rock, "Approach for Evaluation of Lightning Current Distribution on Wind Turbine with Numerical Model," International Conference on Lightning Protection, Estoril, Portugal, 2016.
- [38] R. B. Rodrigues, V. Mendes and J. Catalão, *Protection of interconnected wind turbines against lightning effects: Overvoltages and electromagnetic transients study*, Lisbon: Elsevier, 2012.
- [39] D. Romero, J. Montanyà and A. Candela, *Behaviour of the windturbines under lightning strikes including nonlinear grounding system*, Terrasa, 2004.
- [40] W. Xiaohui, Z. Xiaoqing and Y. Dasheng, *An efficient algorithm of transient responses on wind turbine towers struck by lightning.*, Beijing: Compel, 2008.
- [41] W. Chisholm and K. Srivastava, "Surge response of transmission towers".
- [42] T. Hara and O. Yamamoto, "Modelling of a transmission tower for lightning surge analysis," 1996.
- [43] P. M. J. L. N. A. Gutiérrez R., J. L. Bermúdez, M. Paolone, C. A. Nucci and F. Rachidi, "Nonuniform Transmission Tower Model for," in *IEEE TRANSACTIONS ON POWER*

DELIVERY,, 2004.

- [44] R. B. Rodrigues, V. M. F. Mendes and J. P. S. Catalão, "Analysis of Transient Phenomena Due to a Direct Lightning," 2012.
- [45] Y. M. Hernández, G. Drobnyak and M. Kizilcay, "An Engineering Approach in Modeling Lightning Effects on," Marrakesh, 2010.
- [46] T. Q. Nguye, T. Pham and T. V. Tran, "Electromagnetic transient simulation of lightning overvoltage in a wind farm," in *2013 Electrical Insulation Conference*, Ottawa, 2013.
- [47] B. J. S. E and R. M, "Study of Lightning Current Distribution inside of a Wind Turbine," in *Asia-Pacific International Conference on Lightning*, Nagoya, 2015.
- [48] Y. Yasuda and T. Funabashi, "Transient analysis on wind farm suffered from lightning."
- [49] T. F. Yoh Yasuda, "Equivalent equation of earth resistance for ring electrode of wind turbine.," in *30th International Conference on Lightning Protection*, Cagliari, Italy, 2010.
- [50] H.-C. C. C.-C. K. Jheng-Lun Jiang, "Analysis of transient energy affection for wind farm under lightning," in *Elsevier*, Taipei, Taiwan, 2011.
- [51] N. Malcolm and R. K. Aggarwal, "Transient Overvoltage Study of an Island Wind Farm," 2012.
- [52] K. Yamamoto and S. Sumi, "EMTP models of a Wind Turbine Grounding System," in *International Conference on Lightning Protection*, Shanghai, 2014.
- [53] L. Grcev, "Modeling of Grounding Electrodes Under Lightning Currents," *IEEE TRANSACTIONS ON ELECTROMAGNETIC COMPATIBILITY*, vol. 51, no. 3, pp. 559-570, 2009.
- [54] L. Grcev, "Course on Lightning Protection: High Frequency Grounding.," in *29th International Conference on Lightning Protection*, Uppsala, 2008.
- [55] K. Hirabayashi, "Phase velocity of electromagnetic waves and medium constants," 2001. [Online]. Available: <http://www.mogami.com/e/puzzle/pzl-18.html>. [Accessed 27 August 2018].
- [56] P. Sarajcev, J. Vasilj and D. Jakus, "Monte-Carlo analysis of wind farm lightning-surge transients aided by LINET lightning-detection network data," *Renewable Energy*, 2016.

8. ANNEX I: TOOLS USED IN THE TESTS

In this annex, the models and a brief description of some of the elements used in the practical tests presented in the work will be presented:

Surge generator.

Model:

Surge Generator Model 711. KeyTek Instrument Corporation.

Technical Characteristics:

- Input Voltage: 100/120/220/240V. 50-60Hz.
- $I_{max} = 20A$
- Selectable surges for:
 - Short Branch Circuits: 1.2x50 μs impulse, to 6 kV OCV (Open Circuit Voltage), 8x20 μs impulse to > 3kA SCI (Short-Circuit Current).
5 μs /100 kHz ring wave (damped cosine): to 6kV OCV, 500A SCI.
 - Long Branch Circuits: 5 μs /100 kHz ring wave: to 6kV OCV, 200A SCI.
- Dimensions: 45.1x22.2x54 cm.
- Weight: 29.6 Kg.

Description:

Surge pulses can be produced naturally due to lightning strikes or switching transients, which leads to currents or electromagnetic fields causing high voltage or current transients. Surge voltage can reach several thousands of volts and surge current is seen to reach several thousands of amps.

The Surge Generator Model 711 is a compact, modular set of instrumentation specifically designed for precision surge generation and measurement. The equipment allows the verification and realization of tests through the realization of impulses of current.



Fig. 34: Photo of the Surge Generator Model 711.

Digital Storage Oscilloscope.**Model:**

DSO-X 2014A Oscilloscope: 100 MHz, 4 Analog Channels.

Technical Characteristics:

- Input Voltage: 100 to 120 V, 50/60/400 Hz; 100 to 240 V, 50/60 Hz \pm 10%.
- Channels: 4 analogic channels and 8 digital channels.
- Frequency range: 0.1 Hz to 100 MHz.
- Dimensions: 381x204x142 mm.
- Weight: 3.9 Kg.

Description:

An oscilloscope is an electronic display instrument, widely used in signal electronics for the graphic representation of electrical signals that can vary over time. It presents the values of the electrical signals in the form of coordinates in a screen, in which normally the X axis (horizontal) represents times and the Y axis (vertical) represents tensions. The image thus obtained is called an oscillogram.

In the specific case of this model, it is possible to save the data represented in a pen drive in order to study the data deeply without the necessity of depending on the oscilloscope at all times.

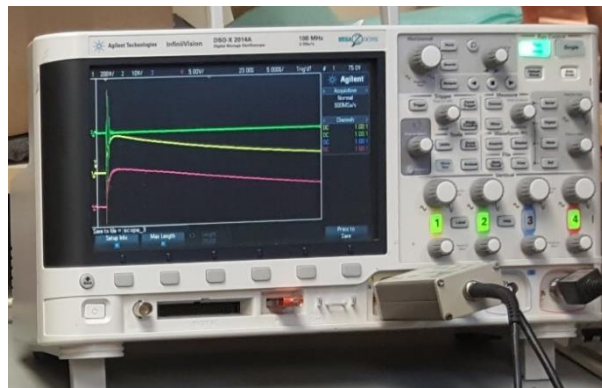


Fig. 35: Photo of DSO-X 2014A Oscilloscope.

High Voltage probe**Model:**

Tektronix P6015A High Voltage Probe.

Technical Characteristics:

- Max Input Voltage: 20 kV DC/40 kV Peak (100 ms Pulse Width).
- Bandwidth: 75 MHz.
- Nominal Length: 10 ft.
- Rise Time: 4.0 ns.
- Loading: 100 Meg 3 pf.
- Compensation Range: 7 to 49 pF.

Description:

The P6015A uses an environmentally safe silicone compound for heavy duty high-performance measurements of voltages over 2.5 kV, being the industry standard. It can measure DC voltages up to 20 kV and pulses up to 40 kV, with a 75 MHz bandwidth to capture faster the high-voltage signals.



Fig. 36: Photo of Tektronix P6015A High Voltage Probe.

9. ANNEX II: GRAPHICS OBTAINED IN THE TESTS

9.1 Test 1:

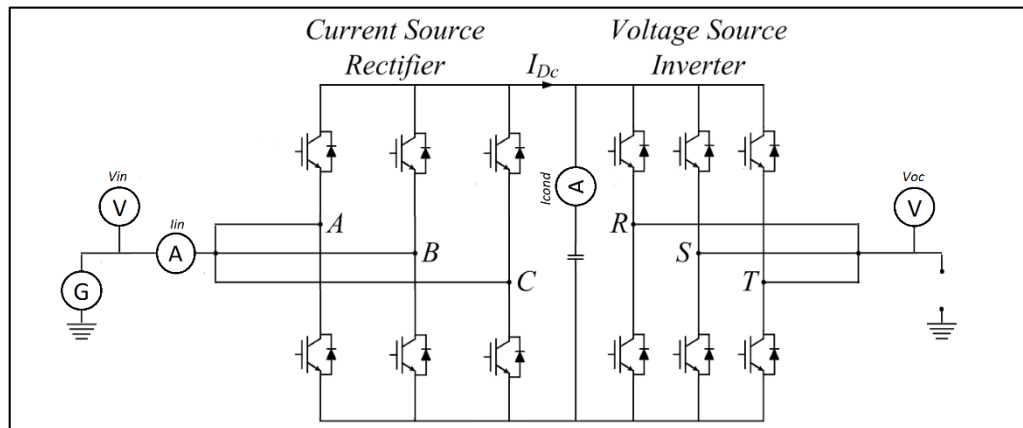


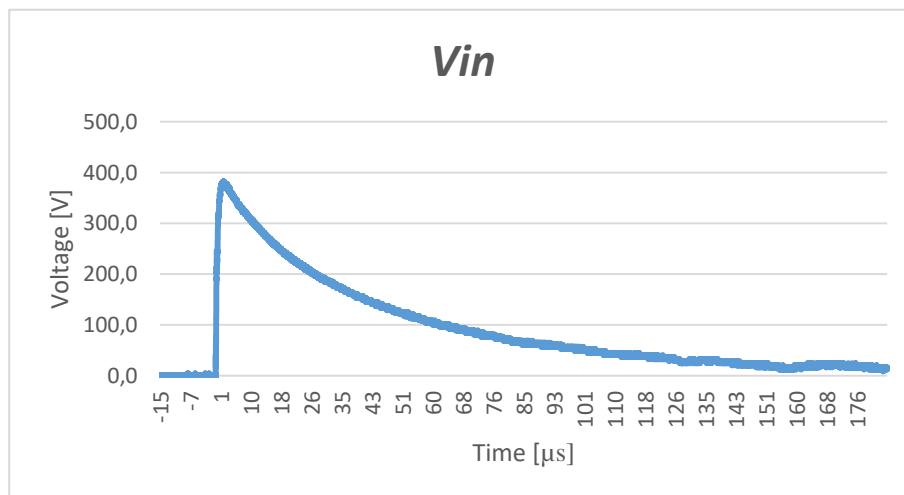
Fig. 37: Test 1 scheme. Open Circuit Test.

Open circuit test with floating capacitor.

Time: 200 μ s and 185 μ s of impulse.

CH1 = V_{in} . CH2 = i_{in} . CH3 = i_{cap} . CH4 = V_{oc} .

CHANNEL 1: V_{in} (200 μ s).

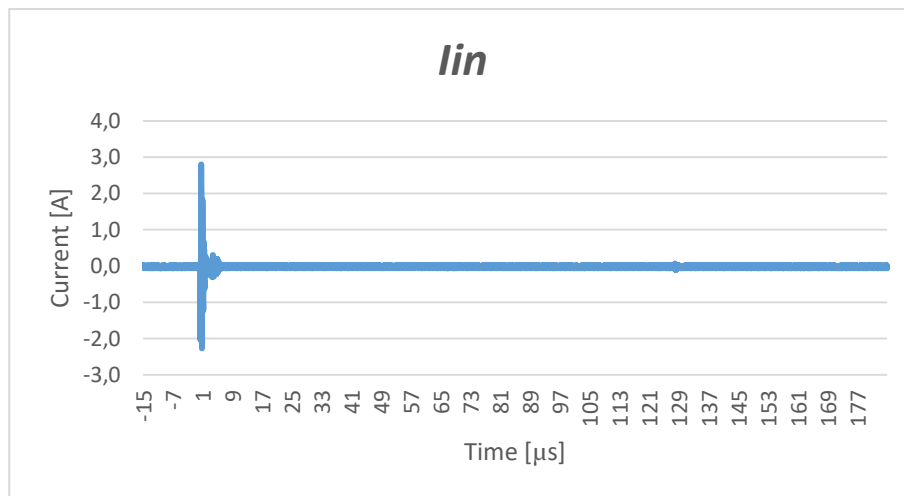


Graphic 9: Input Voltage respect to ground in Test 1.

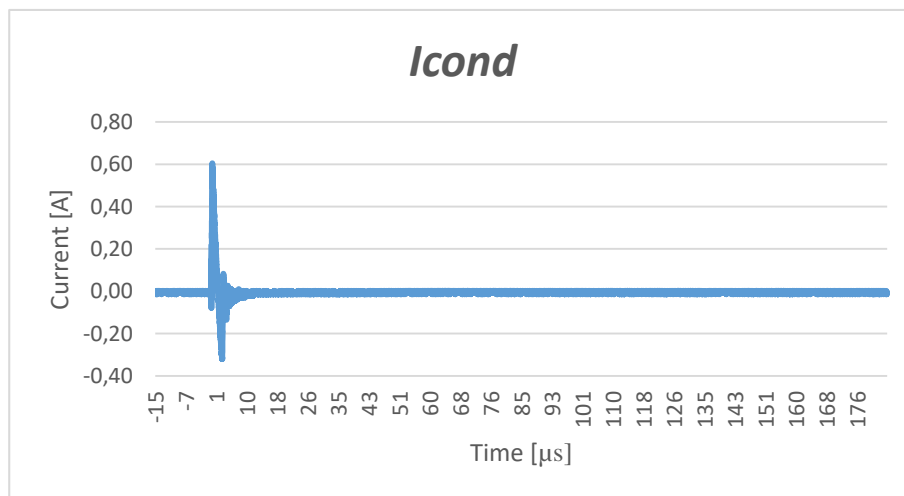
Signal parameters: $V_{max} = 382$ Vp.

$T_1 = 1.86$ μ s.

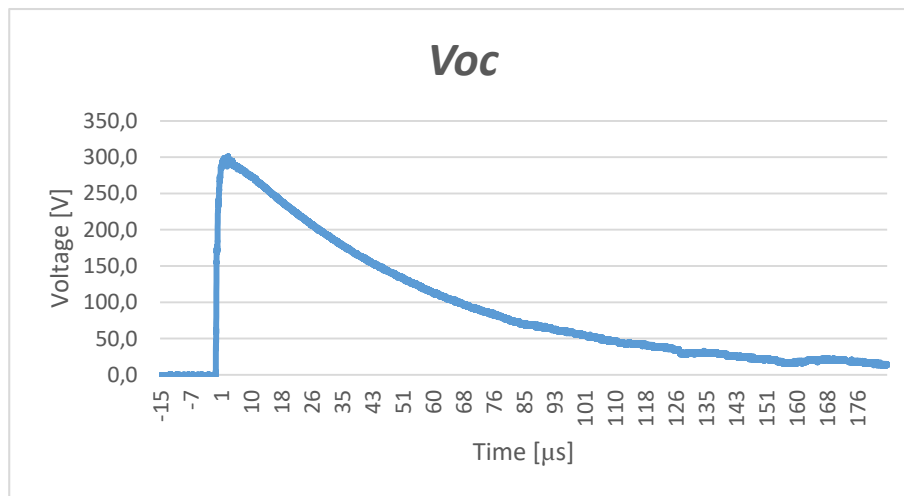
$T_2 = 29.4$ μ s.

CHANNEL 2: lin (200 μ s).*Graphic 10: Input Current in Test 1.*

Signal parameters: $I_{max} = 2.85$ Ap.

CHANNEL 3: Icond (200 μ s).*Graphic 11: Current in the Capacitor in Test 1.*

Signal parameters: $I_{max} = 0.6$ Ip.

CHANNEL 4: Voc (200 μ s).

Graphic 12: Open Circuit Voltage respect to ground in Test 1.

Signal parameters: $V_{max} = 300$ Vp.

$T1 = 3.75$ μ s.

$T2 = 44$ μ s.

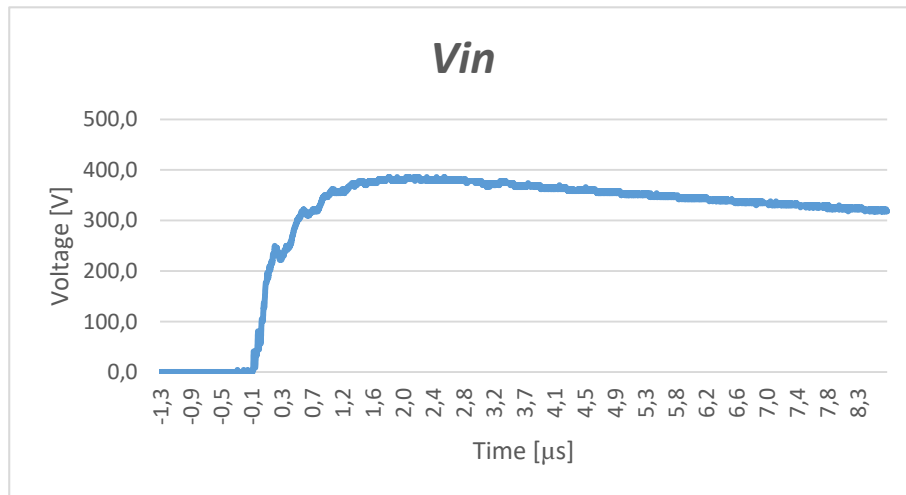
9.2 Test 2

Open circuit test with floating capacitor. Same conditions than in test 1.

Time: 10 μs and 8.65 μs of impulse.

CH1 = V_{in} . CH2 = i_{in} . CH3 = I_{cap} . CH4 = V_{oc} .

CHANNEL 1: V_{in} (10 μs).



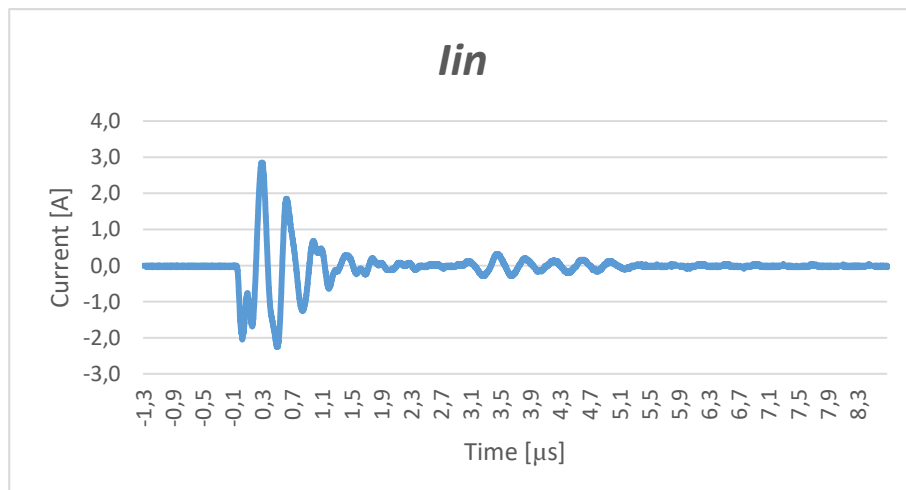
Graphic 13: Input Voltage respect to ground in Test 2.

Signal parameters: $V_{max} = 382 \text{ Vp}$.

$T_1 = 1.86 \text{ } \mu\text{s}$.

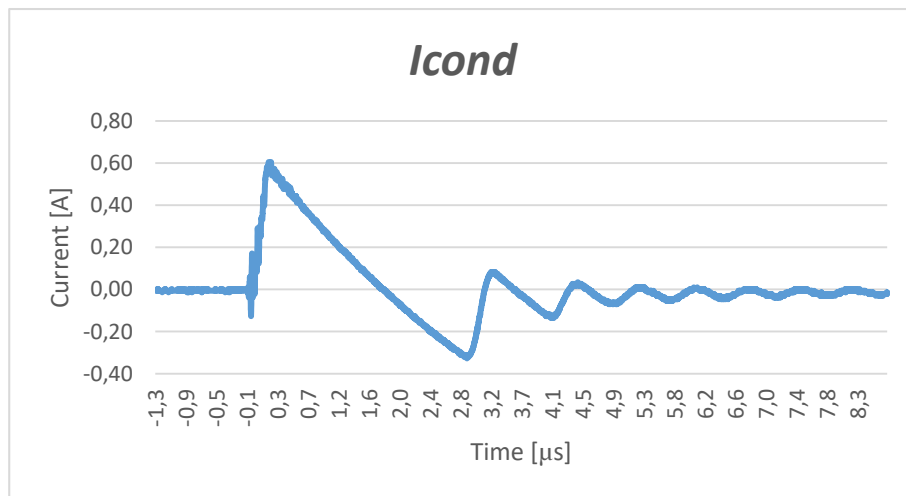
$T_2 = 29.4 \text{ } \mu\text{s}$.

CHANNEL 2: i_{in} (10 μs).

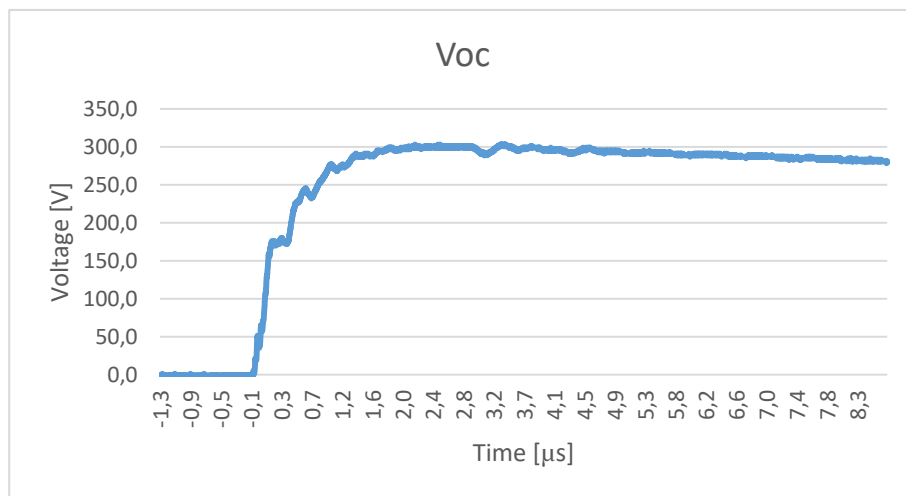


Graphic 14: Input Current in Test 2.

Signal parameters: $I_{max} = 2.85 \text{ Ap}$.

CHANNEL 3: I_{cond} ($10\ \mu s$).*Graphic 15: Current in the Capacitor in Test 2.*

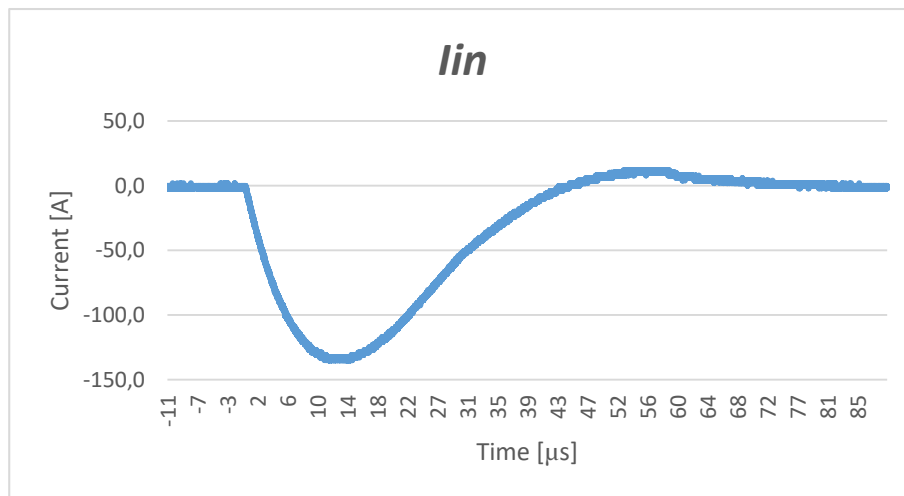
Signal parameters: $I_{max} = 0.6\ A_p$.

CHANNEL 4: V_{oc} ($10\ \mu s$).*Graphic 16: Open Circuit Voltage in Test 2.*

Signal parameters: $V_{max} = 300\ V_p$.

$T_1 = 3.75\ \mu s$.

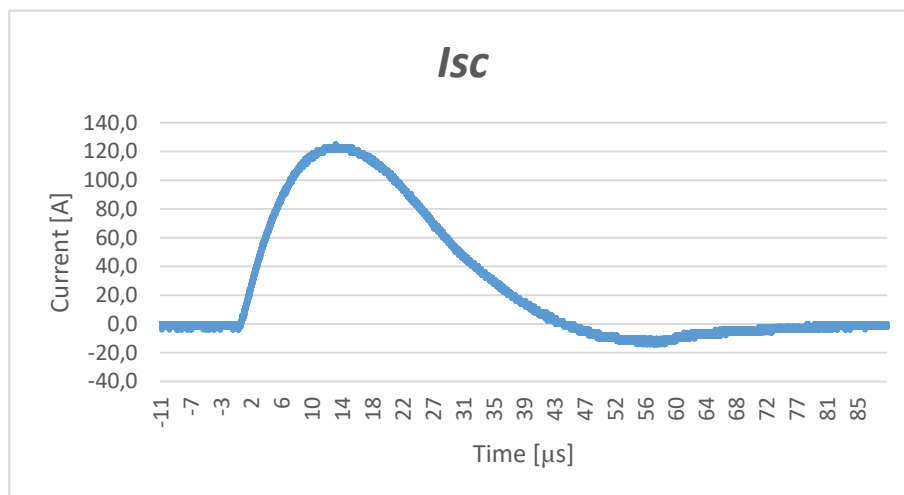
$T_2 = 44\ \mu s$.

CHANNEL 2: i_{lin} (100 μs).*Graphic 18: Input Current in Test 3.*

Signal parameters: $I_{max} = -135$ Ap.

$T1 = 11.5$ μs .

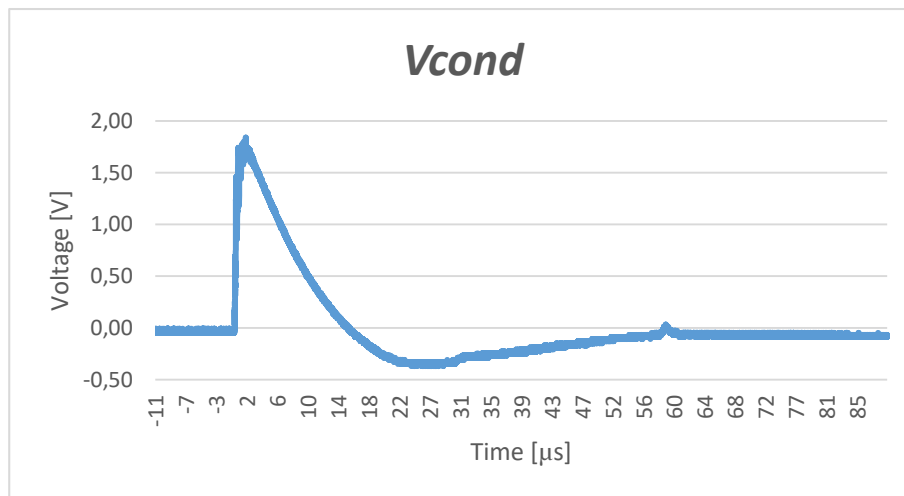
$T2 = 27$ μs .

CHANNEL 3: I_{sc} (100 μs).*Graphic 19: Short-Circuit Current in Test 3.*

Signal parameters: $I_{max} = 123$ Ap.

$T1 = 11.5$ μs .

$T2 = 27$ μs .

CHANNEL 4: Vcond (100 μ s).

Graphic 20: Voltage in the Capacitor respect to ground in Test 3.

Signal parameters: Vmax= 1.78 Vp.

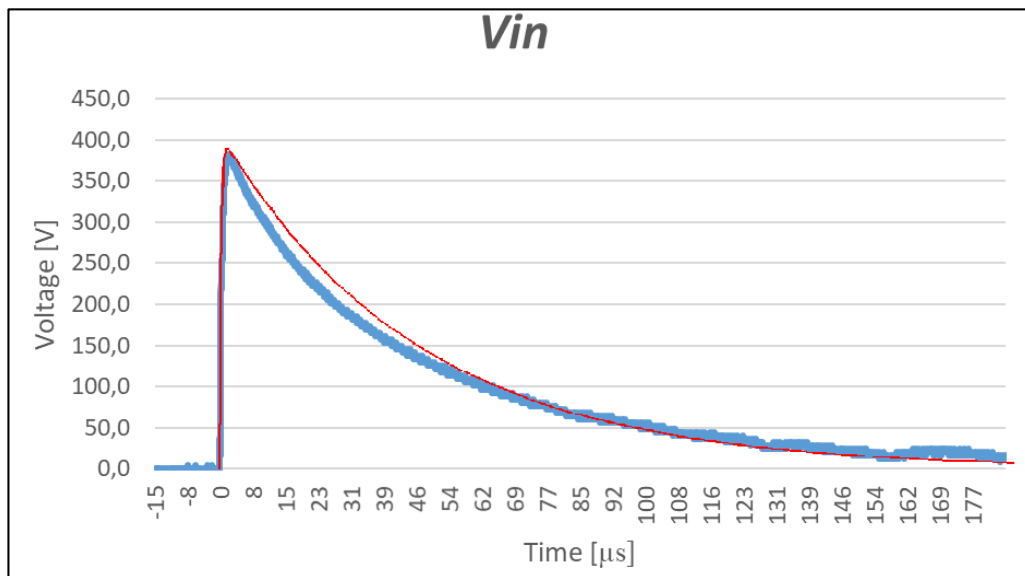
T1= 0.9 μ s.

T2= 6.5 μ s.

10. ANNEX III: COMPARISON BETWEEN THE TEST AND THE FINAL CONVERTER MODEL

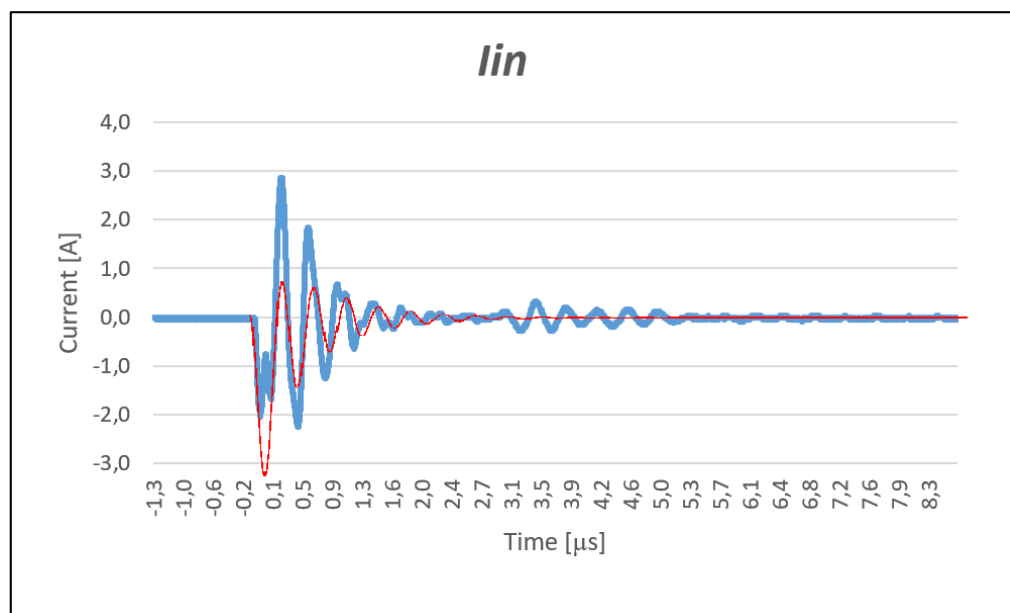
10.1 Open circuit test:

V_{in} (200 μ s).



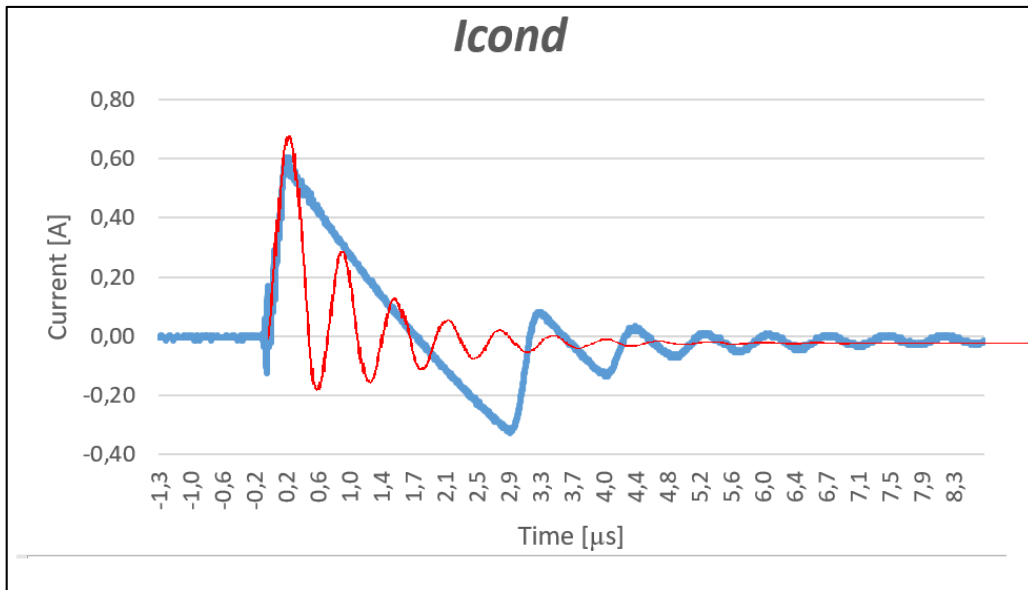
Graphic 21: Comparison of the Input Voltage respect to ground in the Open Circuit test.

i_{in} (10 μ s).



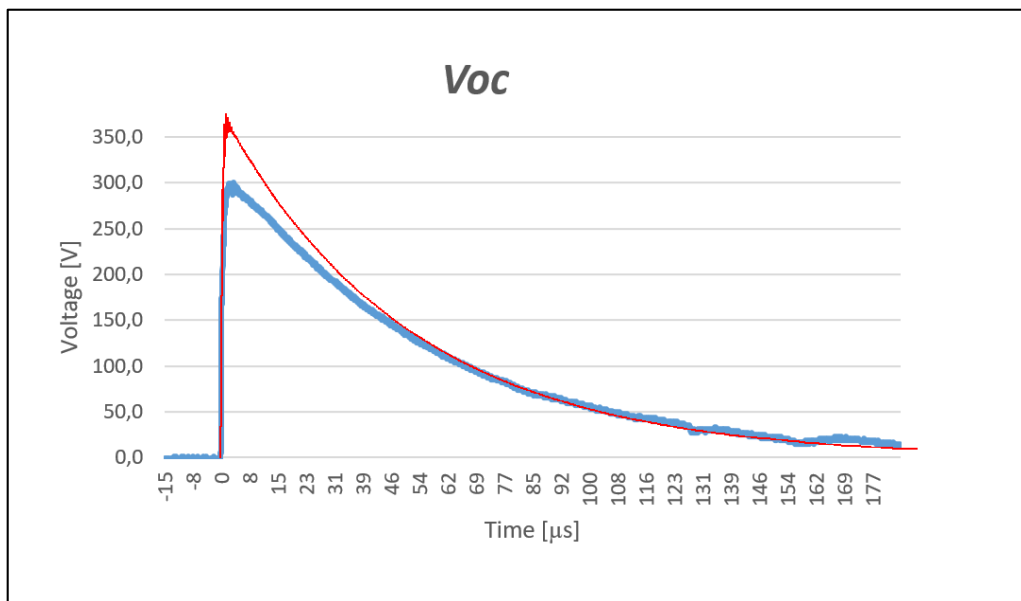
Graphic 22: Comparison of the Input Current in the Open Circuit test.

I_{cond} (10 μ s).



Graphic 23: Comparison of the current in the capacitor in the Open Circuit test.

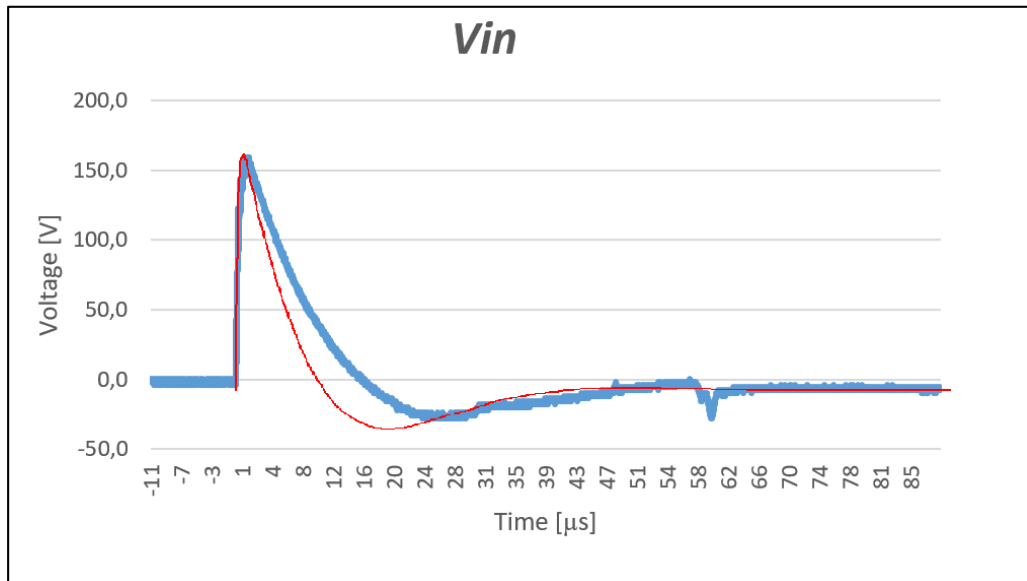
V_{oc} (200 μ s).



Graphic 24: Comparison of the Open Circuit Voltage respect to ground in the Open Circuit test.

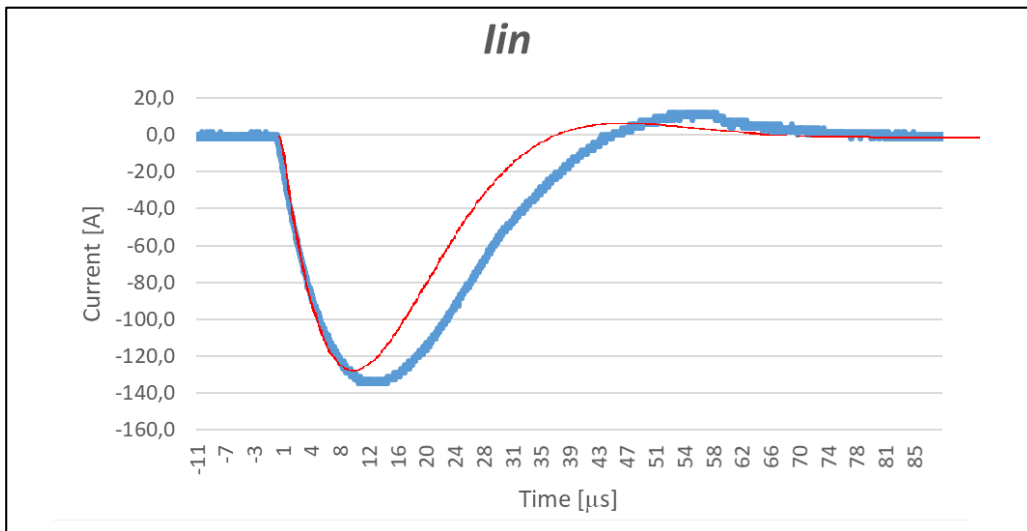
10.2 Short-Circuit Test.

Vin (100 μ s).

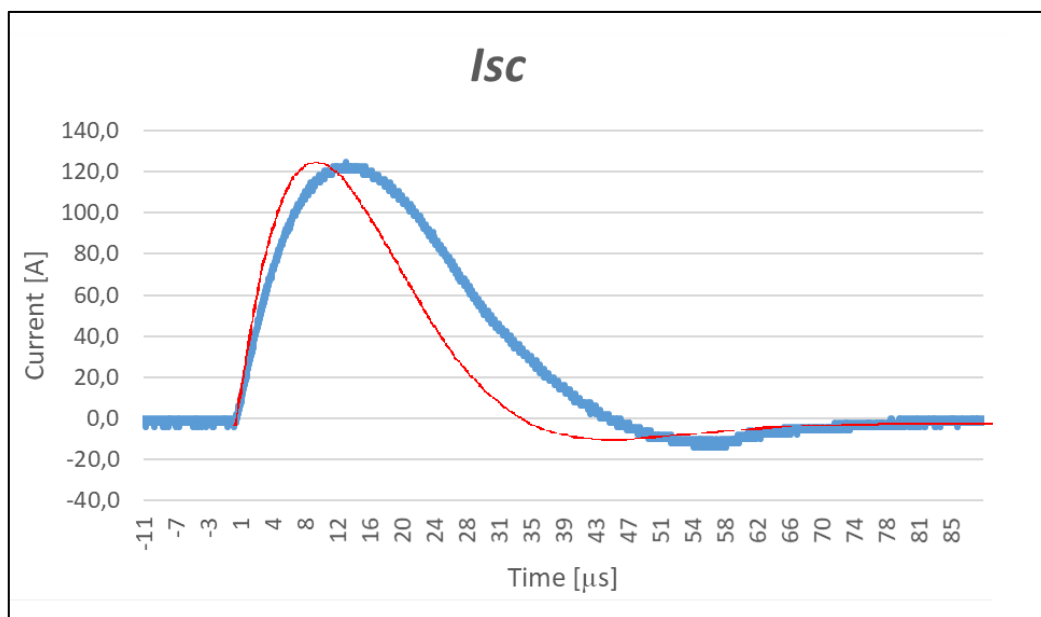


Graphic 25: Comparison of the Input Voltage respect to ground in the Short-Circuit test.

Iin (100 μ s).



Graphic 26: Comparison of the Input Current in the Short-Circuit test.

Isc (100 μ s).

Graphic 27: Comparison of the Short-Circuit current in the Short-Circuit test.

11. ANNEX IV: FINAL SIMULATION

